HHS Public Access

Author manuscript

Sci Signal. Author manuscript; available in PMC 2024 July 04.

Published in final edited form as:

Sci Signal. 2024 April 30; 17(834): eadn4556. doi:10.1126/scisignal.adn4556.

Targeting the postsynaptic scaffolding protein PSD-95 enhances BDNF signaling to mitigate depression-like behaviors in mice

Xin Shi[1,#], **Xiao-zhong Zhou**[1,2,#], **Gang Chen**[3,#], **Wei-feng Luo**[1,#], **Chengyu Zhou**[5], **Tian-ju He**[1], **Mandar T. Naik**[4], **Qin Jiang**[6,*], **John Marshall**[4,*], **Cong Cao**[1,*]

[1]Clinical Research Center of Neurological Disease, The Second Affiliated Hospital of Soochow University, Institution of Neuroscience, Soochow University, Suzhou 215123, China

[2]Department of Orthopedics, the Second Affiliated Hospital of Soochow University, Suzhou, 215004, Jiangsu, China.

[3]Department of Neurosurgery, the First Affiliated Hospital of Soochow University, Suzhou, 215006, Jiangsu, China.

[4]Department of Molecular Biology, Cell Biology & Biochemistry, Brown University, Providence, RI 02912, USA.

[5]Department of Neuroscience, Case Western Reserve University, Cleveland, OH 44106, USA.

[6]The Fourth School of Clinical Medicine, Nanjing Medical University, Nanjing 210029, China

Abstract

Signaling mediated by brain-derived neurotrophic factor (BDNF), which is supported by the postsynaptic scaffolding protein PSD-95, has antidepressant effects. Conversely, clinical depression is associated with reduced BDNF signaling. We found that peptidomimetic compounds that bind to PSD-95 promoted signaling by the BDNF receptor TrkB in the hippocampus and reduced depression-like behaviors in mice. The compounds CN2097 and Syn3 both bind to the PDZ3 domain of PSD-95, and Syn3 also binds to an α-helical region of the protein. Syn3 reduced depression-like behaviors in two mouse models of stress-induced depression; CN2097 had similar but less potent effects. In hippocampal neurons, application of Syn3 enhanced the formation of TrkB-$G\alpha_{i1/3}$-PSD-95 complexes and potentiated downstream PI3K-Akt-mTOR signaling. In mice subjected to chronic mild stress (CMS), systemic administration of Syn3 reversed the CMS-induced, depression-associated changes in PI3K-Akt-mTOR signaling, dendrite complexity, spine density, and autophagy in the hippocampus and reduced depression-like behaviors. Knocking out $G\alpha_{i1/3}$ in hippocampal neurons prevented the therapeutic effects of Syn3, indicating dependence

*Corresponding author. Jqin710@vip.sina.com (Q.J.), John_Marshall@Brown.edu (J.M.), caocong@suda.edu.cn (C.C.).

Author contributions: SX, XZ, GC, WL, MN, QJ, JM, and CC proposed and designed the research. SX, XZ, GC, WL, CZ, TH, MN, QJ, JM, and CC performed the experiments, analyzed the data and organized Figures. QJ, JM, and CC supervised the research. QJ, JM, and CC are responsible for funding acquisition, project administration and revision. SX, XZ, GC, WL, MN, QJ, JM, and CC wrote the manuscript, and all authors discussed the experiments and final manuscript.

[#]These authors contributed equally.

Competing interests: J.M. has filed a patent for the use of poly-arginine derivatives for enhancing brain-derived growth factor to mitigate neurological disorders (U.S. Provisional Application for Patent No. 63/134,059 filed January 5, 2021 and International Application No. PCT/US2022/011283 filed January 5, 2022). All other authors declare that they have no competing interests.

of these effects on the TrkB pathway. The findings suggest that compounds that induce the formation of PSD-95–TrkB complexes have therapeutic potential to alleviate depression.

Introduction

Major depressive disorder (MDD) affects over 17 million U.S. citizens (1), but despite treatment with at least two different antidepressants, 65% of patients remain symptomatic (2). Human studies and animal models support the “neurotrophin hypothesis” of depression proposing that depression is associated with reduced expression or function of brain-derived neurotrophic factor (BDNF) in depressive states (3, 4), which can be alleviated with antidepressant therapy (5–7). The hippocampus is one of several limbic structures implicated in the pathophysiology of depression (8), where BDNF and its high-affinity tropomyosin related kinase B (TrkB) receptor play a critical role in synaptic plasticity (9). Impairment of synaptic plasticity plays a crucial role in the development of depression (10). Recent studies link the pathophysiology of MDD to overactive autophagy (11, 12), and the lysosomal degradation of BDNF (13). BDNF signaling via the phosphatidylinositol-3 kinase (PI3K)-Akt pathway has been reported to suppress autophagy (14, 15), suggesting that the reduced expression of BDNF in depressive states results in hyperactive autophagy and the degradation of synaptic proteins required for synaptic plasticity. In depressed patients, synaptic defects are associated with decreased levels of synaptic proteins, such as the synaptic postsynaptic density protein 95 (PSD-95) (16), and stress can result in hippocampal neuronal atrophy (17).

An advance in the treatment of depression was the finding that a single infusion of a sub-anesthetic dose of ketamine, a N-methyl-D-aspartate (NMDA) receptor blocker, produces rapid antidepressant effects in patients with conventional, treatment-resistant depression (18, 19). BDNF signaling is required for the antidepressant effects of ketamine (20), and esketamine acts to inhibit autophagy through the BDNF-mTOR signaling pathway (11). Using mice, one study found that the antidepressant-like effects of ketamine and its 2R,6R-hydroxynorketamine metabolite involve TrkB binding and promotion of the BDNF signaling pathway. (21). Although ketamine can produce a rapid response in some individuals (22), clinical trial data have raised efficacy and safety issues (23, 24). Thus, there is an urgent need for the development of new anti-depressant drugs for treatment-resistant depression.

Our previous studies show that heterotrimeric $G\alpha_i$ proteins, which transduce G protein-coupled receptor signals, are required for TrkB signaling (25). $G\alpha_i$ knockout mice exhibit severe depressive-like behaviors and decreased dendritic morphology (25). In a stress model of depression, $G\alpha_{i1}$ and $G\alpha_{i3}$ proteins were decreased in the hippocampus and stress-induced depressive-like behaviors were corrected by intra-hippocampal re-expression of $G\alpha_{i3}$ (25). We found that the postsynaptic density protein PSD-95 associates with TrkB to amplify BDNF-induced signaling (26, 27). PSD-95, a master synaptic scaffold protein, contains three PDZ (PSD-95/Discs-large/Zona occludens) domains, of which the PDZ1–2 domains interact directly with the C-termini of NMDAR-GluN2 subunits (28, 29) and also with the C-termini of the TARP auxiliary subunits of AMPA (α-amino-3-hydroxy-5-methyl-4-isoxazole propionic acid) receptors, to regulate AMPAR clustering(30). PSD-95

therapeutic peptides that target the PDZ1–2 domains, such as Tat-NR2B9c, comprising the nine carboxy-terminal amino acids of the N-methyl-d-aspartate receptor (NMDAR) GluN2B subunit fused to the 11-mer HIV-1 Tat protein uncouple PSD-95 from NMDAR neurotoxic signaling (31). The PDZ3 domain interacts with PDZ3 ligands, such as CRIPT, neuroligin, and SynGAP (32), to regulate dendritic arborization and spine number (33). Based on the CRIPT C-terminus (34), a macrocyclic compound, CN2097, was developed that enhanced the association of PSD-95 with TrkB to promote BDNF signaling and correct neurological deficits in a mouse model of Angelman syndrome (27). Additionally, using a structure-based approach we recently developed and reported a cyclic-peptide, called Syn3, that targets the PSD-95 PDZ3 domain and adjoining αC helix to achieve bivalent binding that results in 5-fold stronger affinity compared to CN2097 (35).

Because impaired BDNF signaling has been proposed to underlie the pathophysiology of major depressive disorder (36) and bipolar disorder (37), we examined whether the previously developed PSD-95–binding compounds CN2097 and Syn3 could improve neurobehavioral outcomes in the chronic mild stress (CMS) and corticosterone mouse models of depression. More potently than CN2097, Syn3 enhanced TrkB-$G\alpha_i$-PSD-95 synaptic signaling and mitigated depression-like behaviors. The efficacy of Syn3 on the molecular, cellular, and behavioral levels was dependent on the $G\alpha_{i1}$ and $G\alpha_{i3}$ proteins that transduce signaling from TrkB. Our data show that compounds that engage PSD-95 to enhance BDNF-TrkB signaling may have therapeutic potential to alleviate depression.

Results

CN2097 mitigates depressive-like behaviors in mice

We have previously reported that intraperitoneal injection (i.p.) of CN2097 (10 mg/kg) increases TrkB signaling and facilitates long-term potentiation (26, 27, 38). To investigate the antidepressant-like activity of CN2097, we tested behavioral efficacy in two mouse models of depression, one derived from chronic corticosterone administration (called the CORT model) and the other from chronic mild stress (CMS) (Fig. 1A). In the former, 4- to 5-week-old mice of equal numbers male and female, were subcutaneously (s.c.) injected daily with corticosterone (20 mg/kg) for 21 consecutive days. As expected, chronic corticosterone administration resulted in depression-like behaviors, as indicated by increased immobility time in the forced swim test and tail suspension test, as well as decreased sucrose intake in a sucrose preference test (Fig. 1B). Subsequently, mice were injected i.p. with vehicle, CN2097 (at 1 or 10 mg/kg), or the negative control compound CN5135 (27, 38). Behavioral tests performed 12 hours later showed that injection of the greater dose of CN2097, 10 mg/kg, significantly decreased immobility time in the tail suspension test (Fig. 1B) and the forced swim test (Fig. 1C), and increased sucrose preference (Fig. 1D), suggesting antidepressant-like activity. CN5135 (at 10 mg/kg) and CN2097 (at 1 mg/kg) failed to significantly mitigate depressive-like behaviors in corticosterone-treated mice (Fig. 1B–D). In the CMS model, mice subjected to five weeks of varied and unpredictable mild stressors (hence, also called CUMS) exhibited depression-like behaviors (Fig. 1E–G), which were ameliorated by administration of 10 mg/kg of CN2097, evidenced by shortened immobility time in both the tail suspension test (Fig. 1E) and the forced swim test (Fig. 1F),

and increased sucrose preference (Fig. 1G). Neither CN5135 nor 1 mg/kg of CN2097 had an effect on these depression-like behaviors (Fig. 1, E to G).

Experiment-guided model of Syn3 complex with PDZ3cα

CN2097 consists of a macrocycle moiety that has strong affinity for the PDZ3 domain of PSD-95, but it also binds to the PDZ1 domain (35). We reasoned that a peptidomimetic with selective binding to the PDZ3 domain would augment BDNF signaling without affecting the PDZ1/2 domains which are involved in AMPAR or NMDAR function. The PDZ3 domain shares 44% sequence identity with the PDZ1 domain but uniquely has an unusual additional alpha helix (αC) involved in allosteric peptide binding, that packs against the globular PDZ domain (39). Using a structure-based approach, we previously developed a new peptidomimetic named Syn3 (35). The amino acid sequences of Syn3 and CN2097 (Fig. 2B) consist of a seven-residue, poly-Arg, cell-penetrating peptide attached to the PDZ3-binding cyclic moiety through a disulfide-linkage. The active PDZ3cα binding structure of the Syn3 compound, Syn3*, consists of seven residues derived from the protein SynGAP and six residues based on the CRIPT cyclic peptide (Fig. 2A). Surface plasmon resonance (SPR) experiments showed that Syn3* had a dissociation constant (K_d) of 41 nM, which is roughly a five-fold improvement over CN2097 for binding to the PDZ3cα, and had a higher on-rate (K_a) as well as off-rate (K_d) than CN2097 (Fig. 2B), in agreement with the previous report (35).

As reported previously (35), Syn3 induces strong nuclear magnetic resonance (NMR) perturbation in backbone amide resonances of PDZ3cα. We generated an experiment-guided model of Syn3-bound PDZ3cα (Fig. 2C) using the crystal structure (PDB: 5JXB) as a template in HADDOCK 2.4 web server (40). The model uses ambiguous iterative restraints generated from thirteen non-buried residues of PDZ3cα that showed strong NMR perturbation (35). These residues—Gly^{324}, Phe^{325}, Asn^{326}, Ile^{327}, Val^{328}, Gly^{329}, His^{372}, Glu^{373}, Ala^{376}, Ile^{377}, Lys^{380}, Ile^{404}, and His^{405}—were marked as the active residues, whereas the passive residues were selected automatically by the software. A random conformation of the peptide was generated, and all peptide residues were marked as active. A representative model with the best score was chosen using the Pymol version 1.8 software. This model (Fig. 2C) predicts that the CRIPT cyclic peptide binds the PDZ3 domain between the β2 strand and α helix with three residues Lys^{9}, Thr^{11}, and Val^{13} establishing the critical binding contacts. The SynGAP-derived residues Phe^{4}, Trp^{7}, and Val^{8} were observed to interact with the αC helix residue Ile^{404} (Fig. 2C), which may account for the improved binding affinity of Syn3 for the PDZ3cα domain (Fig. 2B).

Syn3 acts to promote TrkB signaling in hippocampal neurons

To determine whether the increased affinity and specificity of Syn3 for the PSD-95 PDZ3 domain would effectively enhance BDNF-TrkB responses, we performed signaling studies in primary murine hippocampal neurons. Similar to previous studies with CN2097 (26), treatment with Syn3 did not alter BDNF-induced TrkB phosphorylation (Fig. 2D). However, Syn3 at 0.2 μM, a 10-fold lower concentration than the optimal CN2097 concentration (2 μM) (26, 27, 38), significantly enhanced BDNF-induced phosphorylation of Akt (Ser^{473}, Fig. 2E), glycogen synthase kinase 3α/β (GSK3α/β, $Ser^{21/9}$) (Fig. 2E), p70S6K1 (S6K,

at Thr^{389}) and S6 (at Ser$^{235/236}$), and quantified in (Fig. 2, E and F) ($P < 0.001$ vs. BDNF single treatment). Total abundance of TrkB, PSD-95, Akt1, GSK3α/β, S6K and S6 was not significantly altered by Syn3 treatment (Fig. 2D–F). Confirming that Syn3 specifically enhances TrkB signaling, shRNA-induced silencing of TrkB blocked BDNF+Syn3-induced Akt-S6K phosphorylation (Fig. 2G). In the primary hippocampal neurons, Syn3 treatment alone failed to induce TrkB, Akt and S6K phosphorylation (Fig. 2H). Syn3 also had no effect on platelet-derived growth factor (PDGF) receptor and insulin receptor signaling. Treatment with recombinant PDGF or insulin treatment increased Akt and S6K phosphorylation in neurons (Fig. 2I), which was not significantly altered by Syn3 pretreatment (Fig. 2I). In immortalized HT-22 murine hippocampal neuronal cells, Syn3 pretreatment similarly increased BDNF-induced phosphorylation of Akt (Ser^{473}) and S6 (Ser$^{235/236}$) (fig. S1A), leaving TrkB phosphorylation and its protein expression unchanged (fig. S1A).

Syn3 increases BDNF-induced neurite outgrowth and dendritic spine formation in hippocampal neurons

BDNF promotes neurite outgrowth and dendritic spine formation in hippocampal neurons (41). To explore the effect of Syn3 on dendritic architecture, Sholl analysis was performed on green fluorescence protein (GFP)-expressing primary murine hippocampal neurons. A 24h-treatment with BDNF significantly enhanced dendritic complexity and the number of neurite crossings, which was substantially further increased by the addition of Syn3 (Fig. 3, A and B). BDNF increased the number of PSD-95 puncta evaluated by microtubule associated protein 2 (MAP2)-PSD-95 double fluorescence staining (Fig. 3C). The number of PSD-95 puncta per 10 μm dendrite increased further by co-treatment with BDNF and Syn3 (Fig. 3D). Treatment with the TrkB inhibitor K252a or the pan PI3K-Akt-mTOR inhibitor LY294002 blocked the effects of Syn3 demonstrating that Syn3 acts through BDNF-TrkB signaling. BDNF plus Syn3 stimulation of Akt and S6K phosphorylation was blocked by K252a or LY294002 (Fig. 3E). Furthermore, the BDNF+Syn3–induced PSD-95 puncta formation was reversed following treatment with K252a or LY294002 (Fig. 3F).

Synaptic density was determined by counting the number of PSD-95–synaptophysin contacts. Syn3 co-treatment with BDNF significantly increased the number of PSD-95 puncta that colocalized with synaptophysin (Fig. 3, G and H). Compared to BDNF alone, Syn3 co-treatment increased the number of PSD-95–synaptophysin contacts per 10-μm dendrite (Fig. 3H). Co-treatment with K252a or LY294002 blocked the effect of Syn3 on synaptic density (Fig. 3I), supporting the requirement of the TrkB-Akt-mTOR signaling. Examining dendritic spines (Fig. 3, J and K), double staining for F-actin and MAP2 showed that the density of dendritic spines in BDNF-treated hippocampal neurons increased upon Syn3 co-treatment (Fig. 3K), which was reversed by treatment with K252a or LY294002 (Fig. 3L).

Syn3 elicits rapid antidepressant-like efficacy

The CMS depression model was employed to study the antidepressant activity of Syn3 in vivo. Syn3 crosses the blood-brain barrier, as indicated by staining for Alexa Fluor 488-labelled Syn3 in the hippocampus after i.p. injection (fig. S2, A and B). Mice subjected

to five-weeks of continuous CMS stress (Fig. 4A) exhibited depression-like behaviors, with increased immobility time in the tail suspension test (Fig. 4B) and forced swim test (Fig. 4C), and a significantly decreased preference for sucrose (Fig. 4D). Notably, a single 1 mg/kg dose of Syn3 elicited rapid (within 12 hours) antidepressant-like effects (Fig. 4, B to D), reducing immobility time in the tail suspension and forced swim tests (Fig. 4, B and C) and restoring sucrose preference (Fig. 4D).

The hippocampus is implicated in the pathophysiology of depression and is particularly sensitive to stress and glucocorticoids (42), which can result in hippocampal neuronal atrophy (17), characterized by reduced synaptic connections (20). We examined the ability of Syn3 to prevent the reduction in dendritic spine number and synaptic density reported in the hippocampus following CMS (25). Golgi staining revealed that the number of total dendritic spines were substantially decreased in hippocampal CA1 neurons of mice subjected to CMS (Fig. 4E), which was reversed within 12 hours of a single Syn3 injection (Fig. 4E). Dendritic spine density in the CMS group increased following Syn3 administration (Fig. 4E). In CMS-exposed mice, Syn3 restored the number of hippocampal stubby (immature) and mushroom (mature) spines to that observed in control mice (Fig. 4E). The number of long thin (immature) spines was unchanged between the three groups (Fig. 4E).

Examining dendritic density in the CA1 (stratum radiatum subregion) of the hippocampus, the number of PSD-95 puncta, synaptophysin puncta as well as PSD-95-synaptophysin contacts were significantly decreased following CMS (Fig. 4F). The reduction in synaptic density was significantly ameliorated following the injection of Syn3. The density of PSD-95-synaptophysin contacts in the CMS group was increased following Syn3 administration (Fig. 4F). Notably, western blotting showed that synaptophysin and PSD-95 protein expression was decreased in the hippocampal CA1 region of CMS-exposed mice (Fig. 4G), which was reversed with Syn3 administration (Fig. 4G).

To determine whether this manner of systemic Syn3 injection could elicit longer-lasting antidepressant-like effects, behavioral studies in mice after CMS exposure were conducted (Fig. 4H). A 24-hour treatment with Syn3 decreased the duration of immobility in tail suspension and forced swim tests (Fig. 4H) and reinstated sucrose preference (Fig. 4H). As a positive control, we compared the antidepressant-like effects of Syn3 with 7,8-dihydroxyflavone (7,8-DHF), which stimulates TrkB signaling and promotes rapid antidepressant responses (43). A single i.p. injection of 7,8-DHF (10 mg/kg), produced statistically significant antidepressant-like activity in CMS-exposed mice at 24 hours that was comparable to that of Syn3 (Fig. 4H).

The ability of Syn3 to produce rapid antidepressant-like activity was also tested in the corticosterone-induced depression model (Fig. 4I). Similar to CMS-exposed mice, behavioral tests demonstrated that a single i.p. injection of Syn3 (1 mg/kg) (Fig. 4I) rapidly mitigated depression-like behaviors in the corticosterone-injected mice (Fig. 4, J to L). Immobility time in both the tail suspension and forced swim tests were both decreased (Fig. 4, J and K), whereas sucrose preference was significantly increased (Fig. 4L) following Syn3 administration.

Syn3 restores Akt-mTOR activity in the hippocampus of mice exposed to CMS

Defective TrkB-Akt-mTOR activity in the hippocampus is associated with the depression-like behaviors in mice(44). Following CMS, the levels of phosphorylated Akt and S6K were robustly decreased in the hippocampal CA1 region (Fig. 5A), and Syn3 restored Akt and S6K phosphorylation (Fig. 5A). Tissue immunofluorescence staining further revealed downregulation of p-Akt (Fig. 5B) and p-S6 (Fig. 5C) in hippocampal CA1 neurons of stressed mice, which was restored by Syn3 administration (Fig. 5, B and C). Confirming that the rapid antidepressant effects of Syn3 were mediated through the TrkB-Akt-mTOR pathway, bilateral intrahippocampal (CA1) infusion of the TrkB inhibitor K252a or the pan PI3K-Akt-mTOR inhibitor LY294002 reversed the Syn3-induced antidepressant-like effects (Fig. 5, D to F). Additionally, the phosphorylation of Akt-S6K in the prefrontal cortex (PFC) region of CMS-exposed mice was also reduced, which was mitigated following Syn3 administration (fig. S3A).

Our results support that Syn3 enhancement of hippocampal TrkB-Akt-mTOR signaling is the primary mechanism for the Syn3-induced anti-depressant-like effects in mice. To determine if Akt signaling in the hippocampus is sufficient to elicit anti-depressive-like effects we expressed constitutively active Akt in the hippocampal CA1 region. An AAV9-hSyn-S473D-caAkt1-Flag (“caAkt1”) was bilaterally injected into the hippocampal CA1 region and control mice were injected with AAV9-hSyn-vector control (“Vec”). The viral constructs contain the human Synapsin 1 (hSyn) promoter region reported to target transgene expression from adenoviral vectors exclusively to neurons (45). One week following viral injection, mice were exposed to CMS for five weeks. Western blotting analyses (fig. S3B) and immunofluorescence staining (fig. S3C) of the hippocampal CA1 region showed that in mice that were exposed to CMS the expression of caAkt1 substantially increased Akt and S6K phosphorylation compared to vector controls. Behavior confirmed that caAkt1 expression in stressed mice significantly decreased immobility times in the tail suspension and forced swim tests (fig. S3, D and E), and increased sucrose preference (fig. S3F). The control AAV9-hSyn-GFP (green fluorescence protein) was injected into the CA1 region for five weeks, and expression was verified (fig. S3G). Expression of caAkt1 maintained synaptic density following CMS (fig. S4, A to D), prevented synaptophysin and PSD-95 protein downregulation (fig. S4E), and maintained dendritic spine number (fig. S4F). These results support that decreased BDNF-TrkB-Akt signaling contributes to the depression-like behaviors observed in mice following CMS.

Syn3 facilitates BDNF-induced TrkB-PSD-95-$G\alpha_{i1/3}$ complex formation in murine hippocampal neurons

Our previous studies found that PSD-95 binding to TrkB is required for BDNF-induced Akt-mTOR activation (26, 27). Syn3 specifically binds the PDZ3 domain of PSD-95 (Fig. 2C) and, based on previous studies with CN2097 (26) is hypothesized to promote PSD-95-TrkB complex formation. Co-IP results in primary hippocampal neurons confirmed that Syn3 treatment strengthened the BDNF-induced TrkB–PSD-95 association (Fig. 6A). $G\alpha_{i1}$ or $G\alpha_{i3}$ binding to BDNF-activated TrkB is required to mediate TrkB receptor endocytosis and downstream Akt-mTOR activation(25). $G\alpha_{i1}$ and $G\alpha_{i3}$ binding to BDNF-activated TrkB

was potentiated after treatment with Syn3 (Fig. 6A). The expression of TrkB, PSD-95, $G\alpha_{i1}$ and $G\alpha_{i3}$ was unchanged (Fig. 6A).

To further investigate the role $G\alpha_{i1/3}$ in Syn3-mediated TrkB signaling, a viral shRNA approach was utilized to silence $G\alpha_{i1/3}$. Specifically, $G\alpha_{i1}$ and $G\alpha_{i3}$ shRNA-expressing lentiviruses reported in our previous studies (25, 46–48), were co-added to DIV7 primary murine hippocampal neurons ("$G\alpha_{i1/3}$-shRNA") and knockdown efficiency was verified after five days. Compared to control neurons transduced with scramble control shRNA ("shC"), protein expression of $G\alpha_{i1}$ and $G\alpha_{i3}$ was substantially decreased in $G\alpha_{i1/3}$-shRNA neurons (Fig. 6B). Syn3 enhancement of BDNF-induced Akt and S6 phosphorylation was significantly inhibited by $G\alpha_{i1/3}$-knockdown (Fig. 6B), whereas TrkB phosphorylation and total TrkB, Akt1 and S6 expression was unchanged (Fig. 6B). $G\alpha_{i1/3}$-knockdown blocked BDNF+Syn3-induced neurite outgrowth (Fig. 6C), decreased the number of dendritic spines (Fig. 6D) and the number of PSD-95-synaptophysin contacts (Fig. 6E).

To confirm that PSD-95 is required for TrkB-$G\alpha_{i1/3}$ complex formation, PSD-95 was knocked-down in the primary murine hippocampal neurons using two different lentiviral shRNAs (shPSD-95-s1 or shPSD-95-s2, with non-overlapping sequences) (Fig. 6F). Whereas PSD-95 silencing failed to alter BDNF-induced TrkB phosphorylation or $G\alpha_{i1}$, $G\alpha_{i2}$, $G\alpha_{i3}$ and TrkB protein expression (Fig. 6F), it inhibited BDNF+Syn3-induced Akt and S6K phosphorylation (Fig. 6F). These results support that Syn3 binding to PSD-95 facilitates BDNF-induced TrkB:PSD-95:$G\alpha_{i1/3}$ complex formation to enhance downstream Akt-mTOR activation in murine hippocampal neurons. Similar results were observed in primary hippocampal neurons prepared from $G\alpha_{i1/3}$ double knockout (DKO) mice (25), where BDNF+Syn3–induced downstream TrkB signaling (but not PDGF signaling) was blocked (fig. S5, A and B), neurite outgrowth inhibited (fig. S5C), and dendritic spine and synapse formation abolished (fig S5, D and E).

Conditional neuronal knockout of $G\alpha_{i1/3}$ in the hippocampus prevents the antidepressant effects of Syn3

The in vitro results in primary murine hippocampal neurons demonstrate that $G\alpha_{i1/3}$ are absolutely required for TrkB activation of Akt-mTOR signaling, and that Syn3 binding to PSD-95 facilitates BDNF-induced TrkB-PSD-95-$G\alpha_{i1/3}$ complex formation. To confirm the role of $G\alpha_{i1/3}$ in vivo, we performed conditional knockout of both $G\alpha_{i1}$ and $G\alpha_{i3}$ in hippocampal neurons. AAV9-CMV-FLEX-Cas9-U6-sg$G\alpha_{i1}$ and AAV9-CMV-FLEX-Cas9-U6-sg$G\alpha_{i3}$ viruses were bilaterally injected into the CA1 region of the hippocampus of Syn1-Cre C57BL/6J mice (at four-weeks of age), generating hippocampal $G\alpha_{i1/3}$ neuronal conditional knockout ($G\alpha_{i1/3}$-nCKO) mice after three weeks. Compared to control mice injected with AAV9-CMV-FLEX-Cas9-U6-sgC ("sgC"), mRNA and protein levels of $G\alpha_{i1}$ and $G\alpha_{i3}$ were significantly decreased in hippocampal tissues of $G\alpha_{i1/3}$-nCKO mice (Fig. 7, A and B). TrkB protein expression and phosphorylation was unaffected by $G\alpha_{i1/3}$-nCKO (Fig. 7B). Akt and S6K phosphorylation was decreased in the hippocampal tissue of $G\alpha_{i1/3}$-nCKO mice (Fig. 7B), which was confirmed by immunofluorescence (Fig. 7C). A single i.p administration of Syn3 failed to rescue Akt-S6K phosphorylation in hippocampal

CA1 tissues of $G\alpha_{i1/3}$-nCKO mice (Fig. 7A–C) supporting the requirement of $G\alpha_{i1/3}$ for Syn3-mediated enhancement of TrkB signaling.

Behavioral tests confirmed that conditional knockout of $G\alpha_{i1/3}$ in the hippocampal neurons elicited depression-like behavior, increasing immobility time in both the tail suspension and forced swim tests (Fig. 7, D and E) and decreasing sucrose preference (Fig. 7F). Syn3 administration failed to mitigate depressive-like behaviors in $G\alpha_{i1/3}$-nCKO mice (Fig. 7, D to F), demonstrating that $G\alpha_{i1/3}$ are indispensable for Syn3-induced antidepressant activity in mice. $G\alpha_{i1/3}$-nCKO mice had significantly decreased dendritic spine density (Fig. 7G) and the number of postsynaptic PSD-95 puncta (Fig. 7, H and I), presynaptic synaptophysin puncta (Fig. 7, H and J) and PSD-95-synaptophysin contacts (Fig. 7, H and K) were all significantly decreased. Syn3 administration failed to reverse the reduction in dendritic spine density and synaptic density in the $G\alpha_{i1/3}$-nCKO mice (Fig. 7, G to K). Similar results were obtained using a shRNA approach to knockdown both $G\alpha_{i1}$ and $G\alpha_{i3}$ in the hippocampal CA1 region (see fig. S6).

Syn3 ameliorates CMS-induced hyperactive autophagy in hippocampal neurons

Autophagy is critical in maintaining neuronal integrity and synaptic structure(15). The TrkB-Akt-mTOR pathway suppresses autophagy in the hippocampus to facilitate synaptic plasticity and memory enhancement under stress conditions (14). As CMS decreased the phosphorylation levels of Akt and S6K, we tested whether autophagy was dysregulated. Electron microscopy was employed to visualize autophagosomes in the hippocampal CA1 region. Autophagosome vesicles have a characteristic double-membrane, with a smooth outer membrane and an electron-dense granular inner membrane, containing cellular components for degradation. CMS significantly increased the number of autophagosomes within hippocampal neurons (Fig. 8A).

To further monitor autophagic activity in vivo we introduced AAV-mRFP (murine red fluorescence protein)-GFP-LC3 (light chain 3) to detect autophagosome accumulation. Autophagosomes, marked by the presence of both GFP and mRFP fluorescence signals appear as yellow puncta. Following CMS, the average number of yellow puncta was significantly increased in the mouse hippocampal neurons (Fig. 8B). Western blotting, Fig. 8C, confirmed the induction of autophagic flux in hippocampal tissues, evidenced by LC3-II accumulation, Beclin-1 upregulation and p62 degradation (Fig. 8C). Syn3 normalized autophagy as indicated by a reduction in the number of autophagosomes in hippocampal neurons (Fig. 8, A and B) and autophagic flux (Fig. 8C).

Neuronal knockdown of $G\alpha_{i1}$ and $G\alpha_{i3}$ (“$G\alpha_{i1/3}$-nKD”) or conditional knockout (“$G\alpha_{i1/3}$-nCKO”) increased autophagy in the hippocampal CA1 region, showing LC3-II accumulation, Beclin-1 upregulation and p62 degradation (Fig. 8, D and E). Treatment with Syn3, which had failed to restore Akt-mTOR signaling in $G\alpha_{i1/3}$-nKD mice and $G\alpha_{i1/3}$-nCKO mice (figs. S6 and S7), was ineffective in suppressing hyperactive autophagy (Fig. 8, D and E). These results demonstrate for the first time that CMS results in hyperactive autophagy and that Syn3-mediated anti-autophagy activity in hippocampal neurons in mice exposed to CMS requires $G\alpha_{i1/3}$-mediated TrkB-Akt-mTOR activation.

Discussion

Mounting evidence has established the involvement of BDNF-TrkB signaling in the pathophysiology of depression and other mood disorders (6). TrkB signaling is associated with the mechanism of action of the rapid antidepressant actions of ketamine and psychedelic drugs (21, 49). Here, we describe a new peptidomimetic-based drug, Syn3, with anti-depressant-like properties that mimic the rapid-acting effects of ketamine in mouse models of depression. Notably, in contrast to current anti-depressants, Syn3 acts downstream of the receptor TrkB to enhance signaling through pathways that have been linked to rapid antidepressant actions (50).

PSD-95 is a pivotal postsynaptic scaffolding protein which, in addition to regulating AMPAR and NMDAR function, couples with the receptor TrkB to regulate BDNF signaling (26, 51). The development of PSD-95–targeted drugs has focused on its PDZ domains, and we previously reported a peptidomimetic compound, CN2097, that binds the PDZ3 domain of PSD-95 and mitigates deficits in BDNF signaling to restore synaptic plasticity and learning in a mouse model of Angelman syndrome (26, 27). Because there is a strong case for the development of therapeutics that enhance BDNF signaling to alleviate depression, we started by evaluating the antidepressant effects of CN2097 in the CMS and corticosterone mouse models of depression and anxiety (25). Although CN2097 elicited rapid (within 12 hours) anti-depressant-like effects in both models across various behavioral measures, a high dose was required to inhibit depression-like behaviors in mice, likely reflecting the low affinity of the CN2097 cyclic moiety for the PDZ3 domain, as reported in (35). This prompted us to develop higher-affinity compounds targeting the PDZ3 domain of PSD-95, and following rigorous structure-based optimization, a novel Syn3 compound was identified that bound bivalently with high affinity to the PDZ3 domain and the extended αC helix of PSD-95, as previously reported (35).

Syn3 was more potent than CN2097, likewise eliciting rapid antidepressant-like effects in the CMS and corticosterone mouse models of depression but at a dose that was 10-fold lower. Likewise in cultured primary hippocampal neurons, Syn3 more potently augmented BDNF-induced Akt-mTORC1 signaling, including the inhibitory phosphorylation of GSK3α/β, the hyperactivity of which has been linked to mood disorders (52). Silencing or inhibiting TrkB blocked the effects of Syn3 on signaling, dendritic branching, and synapse formation, thus supporting the pathway specificity of Syn3.

The PI3K-Akt-mTOR pathway is implicated in the pathogenesis of depression (53), and drugs exhibiting rapid anti-depressant action have been shown to increase mTOR-dependent synapse formation (54). BDNF acting through mTOR is a negative regulator of autophagy (15), and dendritic autophagy degrades postsynaptic proteins, such as PSD-95, required for synapse formation (55, 56). In agreement with our previous work indicating that deficits in BDNF-mTOR signaling result in increased neuronal autophagy (27), here in hippocampal neurons of mice exposed to CMS we observed aberrantly high autophagic activity with a concomitant decrease in PSD-95 protein levels. Within 12 hours, Syn3 restored Akt and S6K phosphorylation, normalized autophagy, restored PSD-95 expression, and increased the population of mushroom spines, an indicator of synaptic strengthening, and increased

synaptic density. Confirming the role of Akt activity, expression of constitutively active Akt1 in mice exposed to CMS maintained S6K activity and synaptic density and prevented depression-like behaviors.

Syn3 treatment increased the BDNF-induced association between TrkB and PSD-95, demonstrating the importance of the PDZ3 domain of PSD-95 for PSD-95–TrkB complex formation. Syn3 also enhanced $G_{\alpha i1}$ and $G_{\alpha i3}$ binding to BDNF-activated TrkB, which we previously reported to mediate BDNF/TrkB-induced activation of Akt-mTOR signaling (25). In mice, neuronal knockout of $G_{\alpha i1/3}$ in the hippocampus induced similar molecular, cellular, and behavioral effects as those of the depression models and blocked the ability of Syn3 to reverse them. Our observations further demonstrate that heterotrimeric $G_{\alpha i}$ proteins, known to transduce G protein-coupled receptor signals, are required for TrkB downstream signaling, and $G_{\alpha i}$ knockout mice exhibit severe depression-like behaviors (25).

Both typical and fast-acting antidepressants appear to directly bind and allosterically activate TrkB (21). However, treatment with TrkB agonists can be problematic due to toxic side effects resulting from activation of the p75NTR pathway (57) or from a truncated TrkB.T1 isoform that is increased in injury models (58). Promising small-molecule TrkB agonists have been developed that exert beneficial effects in animal models of depression (59), although their effects may not be mediated through TrkB activation (60). Our approach to develop cyclized-peptides that bind intracellularly to PSD-95 circumvents at least these limitations of TrkB agonists (Fig. 8F). Because BDNF signaling is regulated precisely at active synapses, through activity-dependent release to control synaptic plasticity (61, 62), Syn3 is anticipated to specifically enhance synaptic TrkB activity while avoiding non-synaptic TrkB activation and off-target adverse effects. Drugs based on Syn3, that act downstream of NMDAR/AMPAR activity to enhance BDNF-TrkB signaling may provide a promising new approach for the treatment of depression as they combine target selectivity and low toxicity.

Materials and methods

Chemical, reagents, neurons and neuronal cells.

mRNA primers for $G\alpha_{i1/2/3}$ were described in detail in our previous studies(25, 26, 46), as well as primary culture of murine hippocampal neurons from newborn C57BL/6J mice with an equal distribution of male and female (25). Sholl analyses and signaling were performed at DIV12 hippocampal neurons, and synaptic/dendritic density analyses performed in DIV15 hippocampal neurons. LY294002 and K252a were purchased from TOCRIS (Shanghai, China). The vendors of the antibodies are listed in table S1. The viral constructs were obtained from Genechem (Shanghai, China). HT-22 neuronal cells were purchased from Procell (Shanghai, China, RRID: CVCL_0321) and cells maintained under serum-containing DMEM medium with antibiotics. All cell culture reagents were from Gibco (Suzhou, China). All chemicals were provided by Sigma (St. Louis, MO, USA).

Animals.

All animal procedures were approved by the Ethics Committee (SY-BR-2022–0125) and Institutional Animal Care and Use Committees (IACUC) of Soochow University (Suzhou, China). C57BL/6J mice, 4- to 5-week-old, half male and half female, were purchased from Shanghai SLAC Laboratory Animal Co. Ltd (Shanghai, China). The generation of $G\alpha_{i1/3}$ double knockout (DKO) mice by the CRISPR-Cas9 method and KO verification was described in detail in our previous study (25). Mice were maintained under specific pathogen-free (SPF) animal research facilities, with 12-hour dark/12-hour light cycle, 22° ± 1°C temperatures, and ad libitum access to food. For each single animal experiment, an equal number of male and female mice were included, with each gender comprising half of the total sample size, except for cardinal group, there was only a one-mouse difference.

Chronic mild stress (CMS) depression model in mice.

As described (63), the CMS procedure involved the sequential application of various mild and unpredictable stressors, including forced-swimming activities, living space restraint, water and food deprivation, wet sawdust, light/dark cycle reversal, and constant illumination or darkness (63). The CMS procedure lasted for a total of five weeks.

Chronic corticosterone administration.

The adrenal corticosteroid (CAS:50-22-6, product ID: 47130) was purchased Solarbio (Beijing, China). Mice were subcutaneously (s.c.) injected daily with corticosterone (20 mg/kg, emulsified in propylene glycol) between 10:00 and 12:00 a.m. for 21 consecutive days (64, 65), and control mice with vehicle.

Tail suspension test.

A detailed protocol of the tail suspension test was reported previously (25). Briefly, in a soundproof box, mice were suspended by the tail to a hook using adhesive scotch tape. Immobility was defined as the absence of any movement except for those caused by respiration and was recorded by two independent observers blinded to the treatment conditions during a 6-min test period. All behavioral tests were conducted in a quiet and controlled environment to minimize external disturbances. Mice were allowed to acclimate to the testing room for 30 min prior to the experiment and were handled gently to minimize stress.

Forced swim test.

As described previously (25), each mouse was forced to swim in an open cylindrical container (diameter 16 cm; height 25 cm) with a water depth of 20 cm at approximately 25–26°C. Mice were forced to swim for 6 min. Two observers blinded to the treatment conditions recorded the duration of immobility. Immobility was defined as floating motionless in the water, except for small movements necessary to keep the head above water (63, 66). Throughout the experiments, the water temperature remained consistent.

Sucrose preference test.

Mice were exposed to 1% sucrose drinking bottle or water bottle for 12 hours, followed by 24 hours of water deprivation. Each mouse was then exposed to two identical bottles, one containing 1% sucrose solution and the other containing water, for 12 hours. At the end, the volume of water and sugar solution consumed by each mouse was recorded. The preference ratio was calculated as volume of sucrose solution consumed/(volume of sucrose solution consumed + volume of water consumed) × 100 %.

Gene and protein expression detection.

The detailed procedures of co-immunoprecipitation (Co-IP), Western blotting, quantitative real-time PCR (qRT-PCR) and data quantification were described in detail in our previous studies (26, 67). For Western blotting, cultured cells and tissues were homogenized in ice-cold RIPA lysis buffer for 30 min, followed by centrifugation. Total protein concentrations were determined, and equal amounts were loaded onto SDS-PAGE gels and transferred onto PVDF membranes. After blocking with 5% milk in TBS-T, membranes were incubated overnight at 4°C with primary antibodies, then washed and exposed to corresponding HRP-conjugated secondary antibodies. For analysis of multiple proteins on the same blot, membranes were stripped and reprobed, or lysates were run on separate gels (sister gels). Band intensity was always quantified using NIH ImageJ software. For qRT-PCR assays, RNA was extracted using Trizol reagent (Thermo Fisher Scientific) and quantified spectrophotometrically. Reverse transcription to cDNA was carried out using the RevertAid First Strand cDNA Synthesis Kit (Thermo Fisher Scientific). For qPCR, the reaction mixture contained SYBR qPCR Master Mix, forward and reverse primers, and cDNA template. Samples underwent thermal cycling. Gene expression analysis utilized the delta-delta Ct method, with normalization to that of *GAPDH*.

Transit bilateral intrahippocampal injection of virus.

Mice were anesthetized and placed in a stereotaxic frame (RWD Instruments, Shenzhen, China). The described adeno-associated virus (AAV) was bilaterally microinjected into the hippocampal CA1 region (anterior-posterior (AP), −2 mm from bregma; medial-lateral (ML), ±1.5 mm; dorsal-ventral (DV), −1.5 mm) at a flow rate of 0.1 μL/min (0.5 μL/side) using a 10-μL Hamilton syringe (Hamilton Co.). The titer of AAV was 1.0*10^11 vg/mL. AAV-mRFP-GFP-LC3 was purchased from Hanbio Technology (Shanghai, China).

Bilateral intrahippocampal infusion.

For guide cannula implantation, stereotaxic surgeries were performed using the described protocol (68). Briefly, mice were anesthetized and mounted on a stereotaxic instrument (RWD Instruments). Two 26-gauge guide cannulae (10 mm length) were implanted bilaterally into the hippocampus (AP, −2 mm from bregma; ML, ±1.5 mm; DV, −1.5 mm). Cannulae and screws were affixed with dental cement onto the mouse skull. A Hamilton 10-μL microsyringe was utilized to infuse chemicals into each side of the hippocampus, driven by a microdialysis pump (RWD Instruments). K252a (1 ng/side of the hippocampus) and LY294002 (5 ng/side of the hippocampus) were infused at a rate of 0.1 μL/min and a

volume of 0.5 μL per side. The vehicle control for LY294002 and K252a was 17% DMSO in saline.

Neuronal immunofluorescence and spines/puncta quantification in vitro.

The primary murine hippocampal neurons were fixed with 4% paraformaldehyde for 15 min, washed 3x in PBS and incubated with blocking buffer (0.3% Triton X-100 and 5% goat serum) for 1 hour. Neurons were then incubated with primary antibody overnight at 4°C, washed 3x in PBS, then incubated with secondary antibodies for 2 hours at room temperature. Slides were washed 3x in PBS, then were mounted onto microscope slides using ProLong anti-fade reagent with DAPI (Invitrogen). For neurons expressing GFP or F-actin-GFP, anti-GFP antibody was added. For quantification of spines and puncta in vitro, spines/puncta were counted from 10-μm–long dendrite (second-order, about 35 to 45 μm from soma) from randomly-selected neurons. Puncta and spines were counted by three examiners who did not have knowledge of the study group.

Golgi staining.

Golgi staining was performed using Rapid Golgi Stain kit according to the manufacturer's instructions (FD Neuro Technologies, Shanghai, China). Freshly dissected hippocampal CA1 brain slides were immersed in the impregnation solution, comprising equal volumes of Solution-A and Solution-B, and stored at room temperature for two weeks in the dark. Brain tissues were thereafter transferred into Solution-C and stored at room temperature in the dark for another 48 hours. Brains were then sectioned using a Lecia sliding-freezing microtome at a thickness of 100 μm. Brain sections were then stained with Solution-D and Solution-E. Golgi-stained neurons and dendritic segments from hippocampus were imaged by Pannoramic MIDI (3DHIESTECH). Dendritic spine density analysis was performed using ImageJ Fiji (version 1.53). Spines were counted from 30-μm–long dendritic segments (about 50 to 80 μm from soma) of randomly selected neurons.

shRNA-mediated gene silencing in vitro.

The lentiviral GV369 constructs containing the PSD-95 shRNA (shPSD-95-s1 targeting TCACGATCATCGCTCAGTATAAACC/shPSD-95-s2 targeting CGCCGTTTGAGTTCTCCTTTATTTT) or TrkB (targeting CCTTAAGGATAACGAACATTT) were supplied by Genechem (Shanghai, China), each was transduced to HEK-293 cells by Lipofectamine 3000 to generate lentivirus. Virus was added at a multiplicity of infection (MOI) of 12 to cultured neurons at DIV7 that were left for five days, at which point expression of PSD-95 and TrkB in the neurons (DIV12) was examined by Western blotting. The control neurons were infected with a scramble control shRNA lentivirus. Knockdown of $G\alpha_{i1}$ and $G\alpha_{i3}$ in primary murine hippocampal neurons using shRNA lentivirus was described previously (25).

GFP or F-actin-GFP expression in neurons.

For expressing GFP or F-actin-GFP, the primary murine hippocampal neurons at DIV7 were infected with GFP-expressing lentivirus or GFP-tagged F-actin-expressing lentivirus (both from GeneChem, Shanghai, China) at an MOI of 12 for five days.

Synapse labeling in vivo and data quantification.

The detailed protocols for immunohistofluorescence synapse labeling in mouse hippocampal CA1 brain sections and data quantification are as previously described (26). PSD-95 and synaptophysin-immunostained puncta and PSD-95-synaptophysin contacts (co-localization) were counted manually by three examiners who did not have knowledge of the study group.

Neuronal knockdown of $G\alpha_{i1}$ and $G\alpha_{i3}$ in vivo.

The shRNA plasmids targeting the *Gα*$_{i1}$ (*GNAI1*) or *Gα*$_{i1}$ (*GNAI3*) with hSyn promoter of adeno-associated virus 9 (AAV9) (11) were supplied by Genechem. The valid target sequence of $G\alpha_{i1}$ (*GNAI1*) is CCAACAGATGAGTACTTATAT and the valid target sequence of $G\alpha_{i3}$ (*GNAI3*) is CTGTTACGGATGTCATCATTA. The constructs were individually transfected into HEK-293 cells to generate AAV and injected to the mice as reported previously (25). Control mice were injected with AAV9-hSyn scramble control shRNA (“shC”).

Neuronal conditional knockout of $G\alpha_{i1}$ and $G\alpha_{i3}$ in mice.

AAV9-CMV-FLEX-Cas9-U6-sg$G\alpha_{i1}$ and AAV9-CMV-FLEX-Cas9-U6-sg$G\alpha_{i3}$ were both generated and verified by Genechem. Both were co-injected into the hippocampal tissues of the Syn1-Cre C57 mice (4-week-old groups of evenly mixed male and female, obtained from GemPharmatech, Nanjing, China). The sgRNA target sequence of $G\alpha_{i1}$ (*GNAI1*) is ACGCTGCCGAATCGTTCAGC (PAM: TGG) and the sgRNA target sequence of $G\alpha_{i3}$ (*GNAI3*) is CAGGCGTGATTAAACGTTTA(PAM: TGG). Syn1-Cre C57 mice were injected with AAV9-CMV-FLEX-Cas9-U6-sgC (“Cas9-C”).

Forced activation of Akt in vivo.

The constitutively-active mutant Akt1 (caAkt1, S473D) sequence, as reported in our previous study (69), was tagged with Flag in the C-terminal and the sequence was inserted into the AAV9-hSyn vector. The construct was transfected to HEK-293 cells to generate AAV, which was injected bilaterally into mouse hippocampus as reported (25). Control mice were subjected to bilateral intrahippocampal injection of the empty AAV9-hSyn vector (“Vec”).

Electron microscopy.

Following deep anesthesia, the mice underwent transcardial perfusion with a 0.9% saline solution, succeeded by a 2.5% glutaraldehyde solution. Subsequently, the hippocampus was carefully isolated and was subjected to overnight fixation in a 2.5% glutaraldehyde solution at a temperature of 4°C. After a rinse in 0.1 M phosphate buffer, the tissues were postfixed with 1% osmium tetroxide for 5 min at room temperature. Dehydration was carried out with varying concentrations of acetone, culminating in the embedding of the tissues in epoxy resin. Next, ultrathin sections of the tissues were prepared, stained with uranyl acetate and lead citrate, and, ultimately, observed utilizing an FEI Tecnai G2 Spirit Transmission Electron Microscope (FEI Company, a subsidiary of Thermo Fisher Scientific), operated at 80 kV.

AAV-mRFP-GFP-LC3 assay staining.

Mice were anesthetized and positioned on a stereotaxic frame (RWD Instruments, Shenzhen, China) for bilateral microinjection of AAV-mRFP-GFP-LC3 into the hippocampal CA1 region (AP, −2 mm from bregma; ML, ±1.5 mm; DV, −1.5 mm), administering at a flow rate of 0.1 μL/min (0.5 μL/side) using a 10-μL Hamilton syringe (Hamilton Co.), with the AAV titer at 1.0×10^{11} vg/mL. The injection coordinates were described above. Following a 10-min dwell time, the pipettes were retracted, the incision was closed, and the brains were post-fixed overnight in 4% paraformaldehyde at 4°C. Subsequently, the brains underwent dehydration, embedding, and sectioning, with mounted sections examined using a laser scanning confocal microscope.

Statistical analysis.

Data following a normal distribution were presented as mean ± standard deviation (SD), except for the Sholl tests [results expressing as mean ± standard error of mean (SEM)]. The two-tailed unpaired t test was utilized to compare statistical difference between two groups. One-way analysis of variance (ANOVA) plus Tukey's post hoc test were utilized for multiple groups, with two-way ANOVA with Sidak's post hoc test applied for Sholl tests. "Biological repeats" in neurons and cells specifies experiments performed at different times using independently prepared neurons and cells. P values < 0.05 was statistically significant.

Supplementary Material

Refer to Web version on PubMed Central for supplementary material.

Acknowledgments.

We thank Dr. Zai-xiang Tang from Soochow University for validating the utilization of suitable statistical tests in this study.

Fundings:

This work was supported by generous funding from the National Institutes of Health STTR (R41 MH118747), the Harrington Discovery Institute, and the Foundation for Angelman Syndrome Therapeutics. grants from the National Natural Science Foundation of China (82371473, 82171461, 81922025, 82070983), a Project Funded by the Priority Academic Program Development of Jiangsu Higher Education Institutions, the Medical Science and Technology Development Project Fund of Nanjing, and the Natural Science Foundation of Jiangsu Province. The funders had no role in the study design, data collection and analysis, decision to publish, or preparation of the manuscript.

Data and Materials Availability.

All data needed to evaluate the conclusions in the paper are present in the paper and the Supplementary Materials. The newly generated materials are available upon request to the corresponding authors.

References and Notes

1. Kessler RC, Bromet EJ, The epidemiology of depression across cultures. Annu Rev Public Health 34, 119–138 (2013). [PubMed: 23514317]
2. Gill H, Gill B, Rodrigues NB, Lipsitz O, Rosenblat JD, El-Halabi S, Nasri F, Mansur RB, Lee Y, McIntyre RS, The Effects of Ketamine on Cognition in Treatment-Resistant Depression: A

Systematic Review and Priority Avenues for Future Research. Neurosci Biobehav Rev 120, 78–85 (2021). [PubMed: 33242561]

3. Arumugam V, John VS, Augustine N, Jacob T, Joy SM, Sen S, Sen T, The impact of antidepressant treatment on brain-derived neurotrophic factor level: An evidence-based approach through systematic review and meta-analysis. Indian journal of pharmacology 49, 236–242 (2017). [PubMed: 29033483]
4. Sen S, Duman R, Sanacora G, Serum brain-derived neurotrophic factor, depression, and antidepressant medications: meta-analyses and implications. Biol Psychiatry 64, 527–532 (2008). [PubMed: 18571629]
5. Bjorkholm C, Monteggia LM, BDNF - a key transducer of antidepressant effects. Neuropharmacology 102, 72–79 (2016). [PubMed: 26519901]
6. Castren E, Monteggia LM, Brain-Derived Neurotrophic Factor Signaling in Depression and Antidepressant Action. Biol Psychiatry 90, 128–136 (2021). [PubMed: 34053675]
7. Marsden WN, Synaptic plasticity in depression: molecular, cellular and functional correlates. Progress in neuro-psychopharmacology & biological psychiatry 43, 168–184 (2013). [PubMed: 23268191]
8. Price RB, Duman R, Neuroplasticity in cognitive and psychological mechanisms of depression: an integrative model. Mol Psychiatry 25, 530–543 (2020). [PubMed: 31801966]
9. Minichiello L, TrkB signalling pathways in LTP and learning. Nat Rev Neurosci 10, 850–860 (2009). [PubMed: 19927149]
10. Duman RS, Aghajanian GK, Sanacora G, Krystal JH, Synaptic plasticity and depression: new insights from stress and rapid-acting antidepressants. Nature medicine 22, 238–249 (2016).
11. Jiang G, Wang Y, Liu Q, Gu T, Liu S, Yin A, Zhang L, Autophagy: A New Mechanism for Esketamine as a Depression Therapeutic. Neuroscience 498, 214–223 (2022). [PubMed: 35597333]
12. Jin Y, Pang H, Zhao L, Zhao F, Cheng Z, Liu Q, Cui R, Yang W, Li B, Ginseng total saponins and Fuzi total alkaloids exert antidepressant-like effects in ovariectomized mice through BDNF-mTORC1, autophagy and peripheral metabolic pathways. Phytomedicine 107, 154425 (2022). [PubMed: 36137328]
13. Zhang K, Wang F, Zhai M, He M, Hu Y, Feng L, Li Y, Yang J, Wu C, Hyperactive neuronal autophagy depletes BDNF and impairs adult hippocampal neurogenesis in a corticosterone-induced mouse model of depression. Theranostics 13, 1059–1075 (2023). [PubMed: 36793868]
14. Nikoletopoulou V, Sidiropoulou K, Kallergi E, Dalezios Y, Tavernarakis N, Modulation of Autophagy by BDNF Underlies Synaptic Plasticity. Cell metabolism 26, 230–242 e235 (2017). [PubMed: 28683289]
15. Nikoletopoulou V, Tavernarakis N, Regulation and Roles of Autophagy at Synapses. Trends in cell biology 28, 646–661 (2018). [PubMed: 29731196]
16. Leung E, Lau EW, Liang A, de Dios C, Suchting R, Ostlundh L, Masdeu JC, Fujita M, Sanches M, Soares JC, Selvaraj S, Alterations in brain synaptic proteins and mRNAs in mood disorders: a systematic review and meta-analysis of postmortem brain studies. Mol Psychiatry 27, 1362–1372 (2022). [PubMed: 35022529]
17. Watanabe Y, Gould E, McEwen BS, Stress induces atrophy of apical dendrites of hippocampal CA3 pyramidal neurons. Brain research 588, 341–345 (1992). [PubMed: 1393587]
18. Zanos P, Brown KA, Georgiou P, Yuan P, Zarate CA Jr., Thompson SM, Gould TD, NMDA Receptor Activation-Dependent Antidepressant-Relevant Behavioral and Synaptic Actions of Ketamine. J Neurosci 43, 1038–1050 (2023). [PubMed: 36596696]
19. Zhang K, Yao Y, Hashimoto K, Ketamine and its metabolites: Potential as novel treatments for depression. Neuropharmacology 222, 109305 (2023). [PubMed: 36354092]
20. Wohleb ES, Gerhard D, Thomas A, Duman RS, Molecular and Cellular Mechanisms of Rapid-Acting Antidepressants Ketamine and Scopolamine. Current neuropharmacology 15, 11–20 (2017). [PubMed: 26955968]
21. Casarotto PC, Girych M, Fred SM, Kovaleva V, Moliner R, Enkavi G, Biojone C, Cannarozzo C, Sahu MP, Kaurinkoski K, Brunello CA, Steinzeig A, Winkel F, Patil S, Vestring S, Serchov T, Diniz C, Laukkanen L, Cardon I, Antila H, Rog T, Piepponen TP, Bramham CR, Normann C,

Lauri SE, Saarma M, Vattulainen I, Castren E, Antidepressant drugs act by directly binding to TRKB neurotrophin receptors. Cell 184, 1299–1313 e1219 (2021). [PubMed: 33606976]

22. Serafini G, Howland RH, Rovedi F, Girardi P, Amore M, The role of ketamine in treatment-resistant depression: a systematic review. Current neuropharmacology 12, 444–461 (2014). [PubMed: 25426012]
23. Horowitz MA, Moncrieff J, Are we repeating mistakes of the past? A review of the evidence for esketamine. Br J Psychiatry, 1–4 (2020).
24. Sapkota A, Khurshid H, Qureshi IA, Jahan N, Went TR, Sultan W, Alfonso M, Efficacy and Safety of Intranasal Esketamine in Treatment-Resistant Depression in Adults: A Systematic Review. Cureus 13, e17352 (2021). [PubMed: 34447651]
25. Marshall J, Zhou XZ, Chen G, Yang SQ, Li Y, Wang Y, Zhang ZQ, Jiang Q, Birnbaumer L, Cao C, Antidepression action of BDNF requires and is mimicked by Galphai1/3 expression in the hippocampus. Proc Natl Acad Sci U S A 115, E3549–E3558 (2018). [PubMed: 29507199]
26. Cao C, Rioult-Pedotti MS, Migani P, Yu CJ, Tiwari R, Parang K, Spaller MR, Goebel DJ, Marshall J, Impairment of TrkB-PSD-95 signaling in Angelman syndrome. PLoS biology 11, e1001478 (2013). [PubMed: 23424281]
27. Lau KA, Yang X, Rioult-Pedotti MS, Tang S, Appleman M, Zhang J, Tian Y, Marino C, Yao M, Jiang Q, Tsuda AC, Huang YA, Cao C, Marshall J, A PSD-95 peptidomimetic mitigates neurological deficits in a mouse model of Angelman syndrome. Progress in neurobiology 230, 102513 (2023). [PubMed: 37536482]
28. Kornau HC, Schenker LT, Kennedy MB, Seeburg PH, Domain interaction between NMDA receptor subunits and the postsynaptic density protein PSD-95. Science 269, 1737–1740 (1995). [PubMed: 7569905]
29. Niethammer M, Kim E, Sheng M, Interaction between the C terminus of NMDA receptor subunits and multiple members of the PSD-95 family of membrane-associated guanylate kinases. J Neurosci 16, 2157–2163 (1996). [PubMed: 8601796]
30. Schnell E, Sizemore M, Karimzadegan S, Chen L, Bredt DS, Nicoll RA, Direct interactions between PSD-95 and stargazin control synaptic AMPA receptor number. Proc Natl Acad Sci U S A 99, 13902–13907 (2002). [PubMed: 12359873]
31. Ballarin B, Tymianski M, Discovery and development of NA-1 for the treatment of acute ischemic stroke. Acta Pharmacol Sin 39, 661–668 (2018). [PubMed: 29565039]
32. Araki Y, Hong I, Gamache TR, Ju S, Collado-Torres L, Shin JH, Huganir RL, SynGAP isoforms differentially regulate synaptic plasticity and dendritic development. Elife 9, (2020).
33. Omelchenko A, Menon H, Donofrio SG, Kumar G, Chapman HM, Roshal J, Martinez-Montes ER, Wang TL, Spaller MR, Firestein BL, Interaction Between CRIPT and PSD-95 Is Required for Proper Dendritic Arborization in Hippocampal Neurons. Mol Neurobiol 57, 2479–2493 (2020). [PubMed: 32157575]
34. Udugamasooriya G, Saro D, Spaller MR, Bridged peptide macrocycles as ligands for PDZ domain proteins. Org Lett 7, 1203–1206 (2005). [PubMed: 15787467]
35. Naik MT, Naik N, Hu T, Wang SH, Marshall J, Structure-based design of peptidomimetic inhibitors of PSD-95 with improved affinity for the PDZ3 domain. FEBS letters 598, 233–241 (2024). [PubMed: 37904289]
36. Phillips C, Brain-Derived Neurotrophic Factor, Depression, and Physical Activity: Making the Neuroplastic Connection. Neural plasticity 2017, 7260130 (2017). [PubMed: 28928987]
37. Scola G, Andreazza AC, The role of neurotrophins in bipolar disorder. Progress in neuro-psychopharmacology & biological psychiatry 56, 122–128 (2015). [PubMed: 25193130]
38. Marshall J, Szmydynger-Chodobska J, Rioult-Pedotti MS, Lau K, Chin AT, Kotla SKR, Tiwari RK, Parang K, Threlkeld SW, Chodobski A, TrkB-enhancer facilitates functional recovery after traumatic brain injury. Sci Rep 7, 10995 (2017). [PubMed: 28887487]
39. Petit CM, Zhang J, Sapienza PJ, Fuentes EJ, Lee AL, Hidden dynamic allostery in a PDZ domain. Proc Natl Acad Sci U S A 106, 18249–18254 (2009). [PubMed: 19828436]
40. Honorato RV, Koukos PI, Jimenez-Garcia B, Tsaregorodtsev A, Verlato M, Giachetti A, Rosato A, Bonvin A, Structural Biology in the Clouds: The WeNMR-EOSC Ecosystem. Front Mol Biosci 8, 729513 (2021). [PubMed: 34395534]

41. Bennett MR, Lagopoulos J, Stress and trauma: BDNF control of dendritic-spine formation and regression. Progress in neurobiology 112, 80–99 (2014). [PubMed: 24211850]
42. Barfield ET, Gourley SL, Prefrontal cortical trkB, glucocorticoids, and their interactions in stress and developmental contexts. Neurosci Biobehav Rev 95, 535–558 (2018). [PubMed: 30477984]
43. Zhang JC, Yao W, Dong C, Yang C, Ren Q, Ma M, Han M, Hashimoto K, Comparison of ketamine, 7,8-dihydroxyflavone, and ANA-12 antidepressant effects in the social defeat stress model of depression. Psychopharmacology 232, 4325–4335 (2015). [PubMed: 26337614]
44. Abelaira HM, Reus GZ, Neotti MV, Quevedo J, The role of mTOR in depression and antidepressant responses. Life Sci 101, 10–14 (2014). [PubMed: 24582593]
45. Kugler S, Meyn L, Holzmuller H, Gerhardt E, Isenmann S, Schulz JB, Bahr M, Neuron-specific expression of therapeutic proteins: evaluation of different cellular promoters in recombinant adenoviral vectors. Mol Cell Neurosci 17, 78–96 (2001). [PubMed: 11161471]
46. Li Y, Chai JL, Shi X, Feng Y, Li JJ, Zhou LN, Cao C, Li KR, Galphai1/3 mediate Netrin-1-CD146-activated signaling and angiogenesis. Theranostics 13, 2319–2336 (2023). [PubMed: 37153740]
47. Wang Y, Liu YY, Chen MB, Cheng KW, Qi LN, Zhang ZQ, Peng Y, Li KR, Liu F, Chen G, Cao C, Neuronal-driven glioma growth requires Galphai1 and Galphai3. Theranostics 11, 8535–8549 (2021). [PubMed: 34373757]
48. Xu G, Qi LN, Zhang MQ, Li XY, Chai JL, Zhang ZQ, Chen X, Wang Q, Li KR, Cao C, Galphai1/3 mediation of Akt-mTOR activation is important for RSPO3-induced angiogenesis. Protein & cell 14, 217–222 (2023). [PubMed: 37051672]
49. Lin PY, Ma ZZ, Mahgoub M, Kavalali ET, Monteggia LM, A synaptic locus for TrkB signaling underlying ketamine rapid antidepressant action. Cell Rep 36, 109513 (2021). [PubMed: 34407417]
50. Zanos P, Gould TD, Mechanisms of ketamine action as an antidepressant. Mol Psychiatry 23, 801–811 (2018). [PubMed: 29532791]
51. Lau K, Rioult-Pedotti M, Tang S, Appleman M, Zhang J, Tian Y, Marino C, Yao M, Jiang Q, Tsuda A, Huang Y, Cao C, Marshall J, A PSD-95 peptidomimetic mitigates neurological deficits in a mouse model of Angelman Syndrome. (2023).
52. Pardo M, Abrial E, Jope RS, Beurel E, GSK3beta isoform-selective regulation of depression, memory and hippocampal cell proliferation. Genes Brain Behav 15, 348–355 (2016). [PubMed: 26749572]
53. Zhang S, Lu Y, Chen W, Shi W, Zhao Q, Zhao J, Li L, Network Pharmacology and Experimental Evidence: PI3K/AKT Signaling Pathway is Involved in the Antidepressive Roles of Chaihu Shugan San. Drug Des Devel Ther 15, 3425–3441 (2021).
54. Li N, Lee B, Liu RJ, Banasr M, Dwyer JM, Iwata M, Li XY, Aghajanian G, Duman RS, mTOR-dependent synapse formation underlies the rapid antidepressant effects of NMDA antagonists. Science 329, 959–964 (2010). [PubMed: 20724638]
55. El-Husseini AE, Schnell E, Chetkovich DM, Nicoll RA, Bredt DS, PSD-95 involvement in maturation of excitatory synapses. Science 290, 1364–1368 (2000). [PubMed: 11082065]
56. Kallergi E, Daskalaki AD, Kolaxi A, Camus C, Ioannou E, Mercaldo V, Haberkant P, Stein F, Sidiropoulou K, Dalezios Y, Savitski MM, Bagni C, Choquet D, Hosy E, Nikoletopoulou V, Dendritic autophagy degrades postsynaptic proteins and is required for long-term synaptic depression in mice. Nat Commun 13, 680 (2022). [PubMed: 35115539]
57. Josephy-Hernandez S, Jmaeff S, Pirvulescu I, Aboulkassim T, Saragovi HU, Neurotrophin receptor agonists and antagonists as therapeutic agents: An evolving paradigm. Neurobiol Dis 97, 139–155 (2017). [PubMed: 27546056]
58. Yanpallewar SU, Barrick CA, Buckley H, Becker J, Tessarollo L, Deletion of the BDNF truncated receptor TrkB.T1 delays disease onset in a mouse model of amyotrophic lateral sclerosis. PLoS One 7, e39946 (2012). [PubMed: 22761934]
59. Zagrebelsky M, Korte M, Are TrkB receptor agonists the right tool to fulfill the promises for a therapeutic value of the brain-derived neurotrophic factor? Neural Regen Res 19, 29–34 (2024). [PubMed: 37488840]

60. Boltaev U, Meyer Y, Tolibzoda F, Jacques T, Gassaway M, Xu Q, Wagner F, Zhang YL, Palmer M, Holson E, Sames D, Multiplex quantitative assays indicate a need for reevaluating reported small-molecule TrkB agonists. Sci Signal 10, (2017).

61. Wang CS, Kavalali ET, Monteggia LM, BDNF signaling in context: From synaptic regulation to psychiatric disorders. Cell 185, 62–76 (2022). [PubMed: 34963057]

62. Leal G, Bramham CR, Duarte CB, BDNF and Hippocampal Synaptic Plasticity. Vitam Horm 104, 153–195 (2017). [PubMed: 28215294]

63. Ducottet C, Griebel G, Belzung C, Effects of the selective nonpeptide corticotropin-releasing factor receptor 1 antagonist antalarmin in the chronic mild stress model of depression in mice. Progress in neuro-psychopharmacology & biological psychiatry 27, 625–631 (2003). [PubMed: 12787849]

64. Lopes IS, Oliveira ICM, Capibaribe VCC, Valentim JT, da Silva DMA, de Souza AG, de Araujo MA, Chaves RC, Gutierrez SJC, Barbosa Filho JM, Macedo DS, de Sousa FCF, Riparin II ameliorates corticosterone-induced depressive-like behavior in mice: Role of antioxidant and neurotrophic mechanisms. Neurochemistry international 120, 33–42 (2018). [PubMed: 30041016]

65. Bai Y, Song L, Dai G, Xu M, Zhu L, Zhang W, Jing W, Ju W, Antidepressant effects of magnolol in a mouse model of depression induced by chronic corticosterone injection. Steroids 135, 73–78 (2018). [PubMed: 29555480]

66. Zhou QG, Hu Y, Hua Y, Hu M, Luo CX, Han X, Zhu XJ, Wang B, Xu JS, Zhu DY, Neuronal nitric oxide synthase contributes to chronic stress-induced depression by suppressing hippocampal neurogenesis. Journal of neurochemistry 103, 1843–1854 (2007). [PubMed: 17854383]

67. Cao C, Huang X, Han Y, Wan Y, Birnbaumer L, Feng GS, Marshall J, Jiang M, Chu WM, Galpha(i1) and Galpha(i3) are required for epidermal growth factor-mediated activation of the Akt-mTORC1 pathway. Science signaling 2, ra17 (2009). [PubMed: 19401591]

68. Huang WL, Hsiung MH, Dai W, Hu SS, Rottlerin, BDNF, and the impairment of inhibitory avoidance memory. Psychopharmacology 238, 421–439 (2021). [PubMed: 33146738]

69. Yao J, Wu XY, Yu Q, Yang SF, Yuan J, Zhang ZQ, Xue JS, Jiang Q, Chen MB, Xue GH, Cao C, The requirement of phosphoenolpyruvate carboxykinase 1 for angiogenesis in vitro and in vivo. Science advances 8, eabn6928 (2022). [PubMed: 35622925]

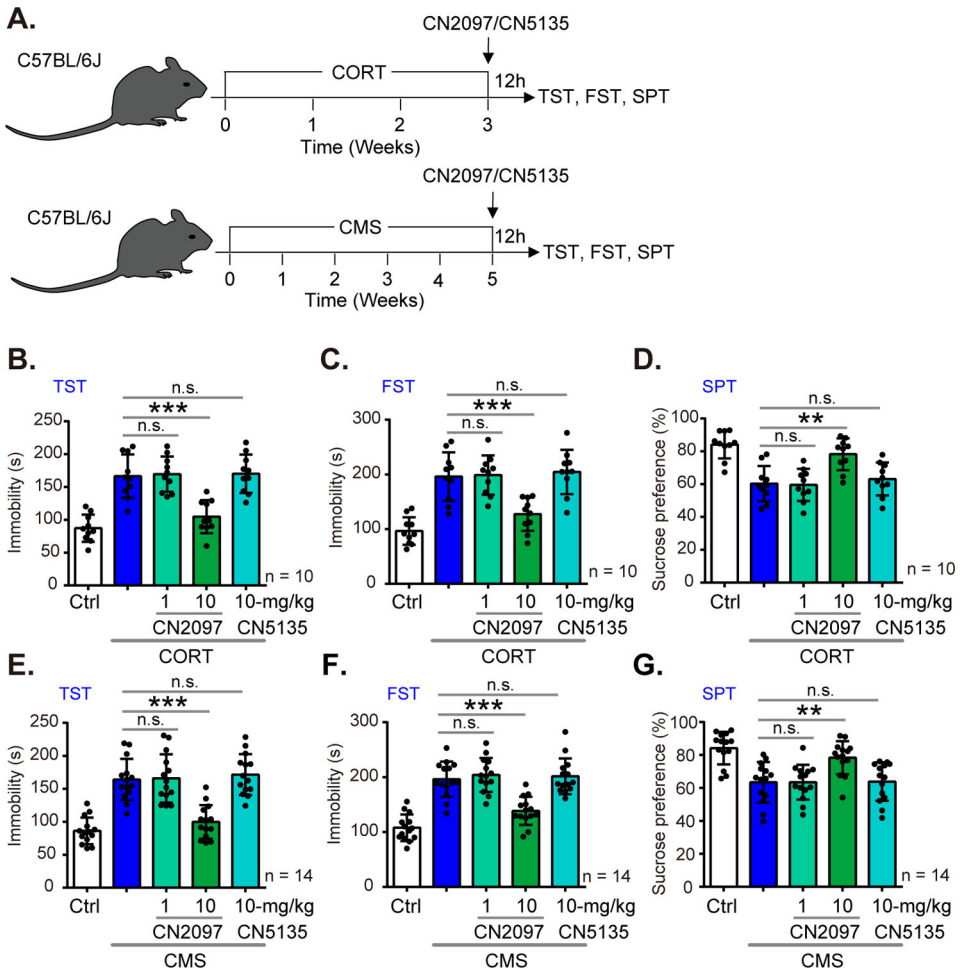

Figure 1. CN2097 mitigates depression-like behaviors in mice.

(**A**) Schematic diagram of the animal protocol. (**B to G**) Assessment of CN2097 on antidepressant-like behaviors in corticosterone model (B-D) and CMS model (E-G) mice. C57BL/6J mice were subcutaneously (s.c.) injected with corticosterone (CORT, 20 mg/kg) daily for 21 days (B-D) or subjected to chronic mild stress (CMS) for five consecutive weeks (E-G), thereafter CN2097 (1 or 10 mg/kg) or CN5135 (10 mg/kg) were administered i.p.. After 12 hours, tail suspension (TST; B and E), forced swim (FST; C and F) and sucrose preference (SPT; D and G) behavioral tests were performed. Data are presented as mean ± standard deviation (SD) from, n = 10 (B to D) or 14 (E to G) mice per group. $^{**}P < 0.01$, $^{***}P < 0.001$, "n.s." not significant ($P > 0.05$) by one-way ANOVA plus Tukey's post hoc test.

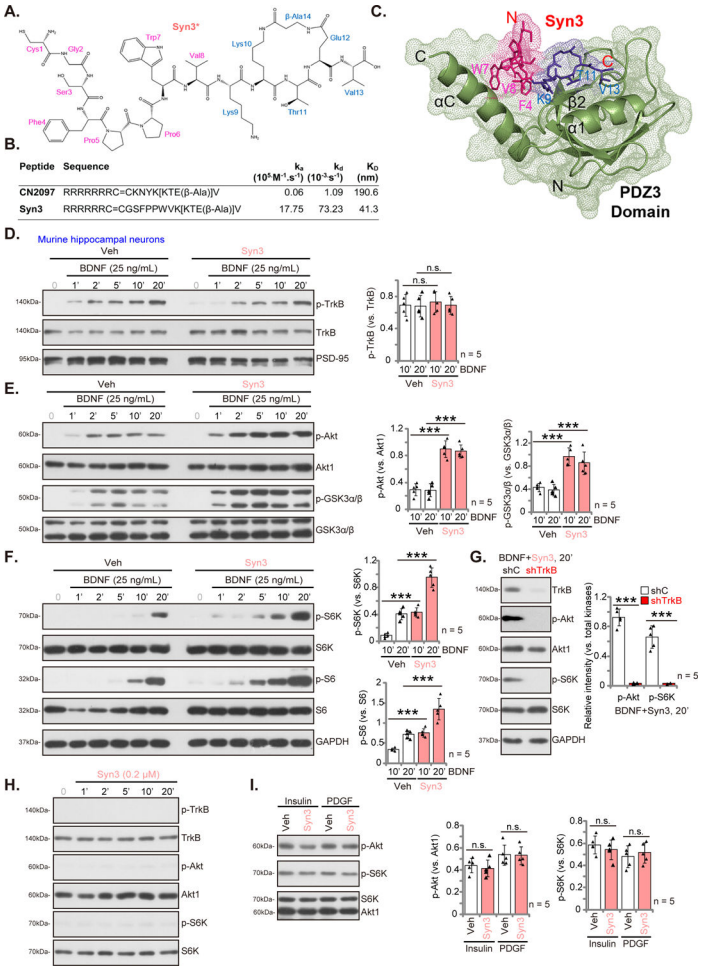

Figure 2. Syn3 promotes TrkB signaling in hippocampal neurons.

(**A**) Structure of the active cyclic peptide Syn3*. (**B**) Comparison of the amino acid sequences of Syn3 and CN2097 and SPR measurements for binding to the PSD-95 PDZ3cα domain. (**C**) Nuclear magnetic resonance (NMR) showing the binding of Syn3 with the PDZ3cα fragment of PSD-95. (**D to F**) Effect of Syn3 on TrkB signaling. Primary murine hippocampal neurons were pre-treated with Syn3 (0.2 μM) or PBS vehicle control (“Veh”) for 20 min, followed by BDNF (25 ng/mL) treatment for 1 to 20 min. Immunoblotting and analysis assessing the effect of Syn3 on the relative abundance of the indicated phosphorylated proteins in primary murine hippocampal neurons that were pre-treated with Syn3 (0.2 μM) or PBS vehicle control (“Veh”) for 20 min, followed by BDNF (25 ng/mL) treatment for 1 to 20 min. (**G**) Role of TrkB in the signaling effects of Syn3. Primary murine hippocampal neurons were treated with a lentiviral TrkB shRNA (“shTrkB”) or lentiviral scramble control non-sense shRNA (“shC”) for five days, after which neurons were stimulated with BDNF (25 ng/mL) for 20 min after a 20-min pretreatment with Syn3 (0.2 μM) (“BDNF+Syn3”). TrkB signaling was analyzed in whole cell lysates by immunoblotting for the indicated proteins. (**H**) Representative immunoblotting to assess TrkB-Akt-S6K signaling in primary murine hippocampal neurons treated with Syn3 (0.2 μM) alone for 1 to 20 min and were analyzed by the listed proteins in total lysates. (**I**)

Immunoblotting analysis to assess the effect of Syn3 on insulin- or PDGF-induced Akt-S6K signaling. Primary murine hippocampal neurons were pre-treated with Syn3 (0.2 μM) or vehicle for 20 min, followed by treatment with insulin (1 μg/mL) or PDGF-BB (25 ng/mL) for 20 min. Data are presented as mean ± SD; in (D to I), n = 5 biological repeats. ***$P <$ 0.001. “n.s.” not significant ($P > 0.05$) by one-way ANOVA plus Tukey’s post hoc test (D to F) or Student’s t test (G and I).

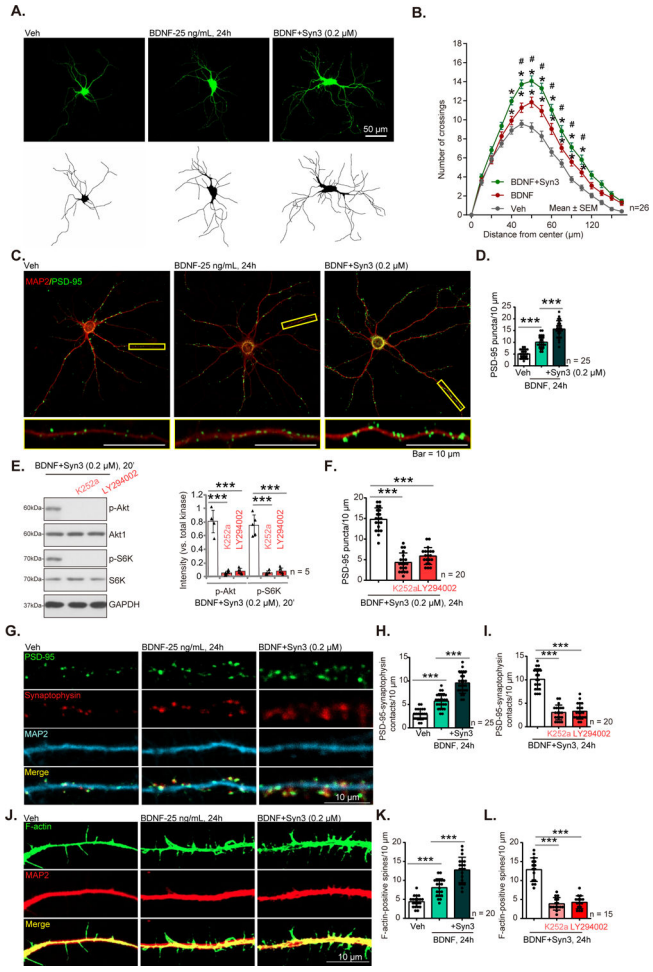

Figure 3. Syn3 enhances BDNF-induced neurite outgrowth and dendritic spine formation in hippocampal neurons.

(**A**) Representative neuronal morphology of GFP-expressing primary murine hippocampal neurons pre-treated with Syn3 (0.2 μM) or PBS vehicle control (“Veh”) for 20 min, followed by BDNF (25 ng/mL) treatment for 24 hours. Scale bar = 50 μm. (**B**) Sholl analyses demonstrates that Syn3 increases neuronal complexity and the number of neurite crossings (n = 26 neurons). (**C and D**) Syn3 increases the number of PSD-95 puncta. Primary hippocampal neurons were pre-treated with Syn3 (0.2 μM) or PBS vehicle control (“Veh”) for 20 min, followed by BDNF (25 ng/mL) treatment for 24h. Representative images of immunofluorescence staining for PSD-95 (green fluorescence) and MAP2 (red fluorescence) are shown (C), scale bars = 10 μm, and the number of PSD-95 puncta per 10 μm dendrite from n = 25 neurons over five independent experiments are quantified in (D). (**E to L**) Inhibition of TrkB or PI3K-Akt blocks Syn3 effects on Akt-S6K signaling (E), PSD-95 puncta formation (F, quantified per 10 μm dendrite, n = 20 neurons per group over five independent experiments), synaptic density (G to I) and spine formation (J to L). Hippocampal neurons were first treated with either the TrkB inhibitor K252a (200 nM) or the pan PI3K-Akt-mTOR kinase inhibitor LY294002 (1 μM) for 1 hour; then Syn3 (0.2 μM) for 20 min, followed by BDNF (25 ng/mL) for 20 min for the immunoblotting in (E, n = 5 biological repeats) or 24 hours for immunofluorescence analysis (F to L). For synaptic

density, representative dendritic staining for PSD-95 (green), synaptophysin (red) and MAP2 (cyan) is shown (G), and PSD-95-synaptophysin contacts per 10 μm dendrite was quantified (H, n = 25 neurons per group over five independent experiments), also in the presence of K252a or LY294002 (I, n = 20 neurons per group over five independent experiments). For spine density, representative F-actin-GFP positive hippocampal dendrites are shown (J); the number of F-actin-GFP positive spines per 10 μm dendrite was quantified (K, n = 20 neurons per group over five independent experiments), also in the presence of K252a or LY294002 (L, n = 15 neurons per group over five independent experiments). In (G and J), scale bars = 10 μm. Data presented as mean ± SEM (B) or SD (D-L). $*P < 0.05$ vs. "Veh" group (A); $^{\#}P < 0.05$ vs. "BDNF" only treatment (A); $***P < 0.001$ (D-L), by two-way ANOVA with Sidak's post hoc test (**B**) or one-way ANOVA plus Tukey's post hoc test (D, E, F, H, I, K and L).

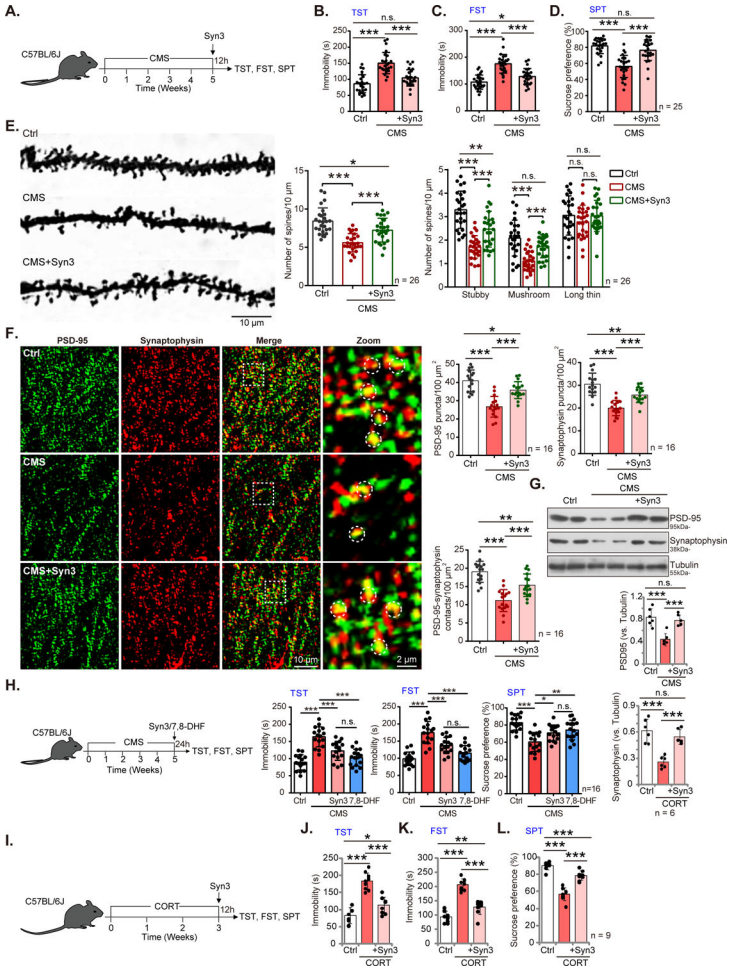

Figure 4. Syn3 mitigates depression-like behaviors in mice.

(**A**) Schematic showing C57BL/6J mice subjected to 5-week of CMS exposure were i.p.-injected with Syn3 (1 mg/kg). (**B to D**) Effect of Syn3 depression-like phenotypes following CMS. Behavioral tests—tail suspension test (TST, B), forced swim test (FST, C) and sucrose preference test (SPT, D)—were performed after 12 hours in n = 25 mice per group. (**E**) Effect of Syn3 on the CMS-induced reduction in dendritic spines. Representative images (scale bar 10 μm) showing Golgi staining of dendritic spines in hippocampal CA1 neurons from mice described in (A). The number of stubby, mushroom, and thin spines were counted from 30-μm-long dendritic segments located ~50–80 μm from the soma of n = 26 randomly selected neurons from N = 7 mice per group. (**F**) Effect of Syn3 on the CMS-induced reduction in synaptic contacts. Representative low- and high-magnification images (scale bars = 10 and 2 μm) of PSD-95 and synaptophysin puncta in hippocampal CA1 brain sections (stratum radiatum subregion) from mice exposed to CMS. PSD-95-positive clusters, synaptophysin-positive clusters, and PSD-95–synaptophysin contacts were quantified from random views from sections from n = 16 mice per group. (**G**) Effect of Syn3 on PSD-95 and synaptophysin protein expression in hippocampal CA1 tissues of mice exposed to CMS. Immunoblotting of tissues of n = 6 mice per group, described in (A), were analyzed. (**H**) C57BL/6J mice with 5 weeks of CMS exposure were injected i.p. with Syn3 (1 mg/kg)

or 7,8-DHF (10 mg/kg). After 24 hours, behavioral tests were performed, as in (B to D), in n = 16 mice per group. (**I to L**) Effect of Syn3 on depression-like phenotypes in the corticosterone model. C57BL/6J mice were injected with corticosterone (s.c., 20 mg/kg) daily for 21 consecutive days. Thereafter, Syn3 (1 mg/kg, i.p.) was administered, and 12 hours later performance on behavioral tests, as described in (B to D), was assessed in n = 9 mice per group. Data are presented as mean ± SD. $*P < 0.05$, $**P < 0.01$, and $***P < 0.001$; "n.s." not significant ($P > 0.05$); by one-way ANOVA plus Tukey's post hoc test.

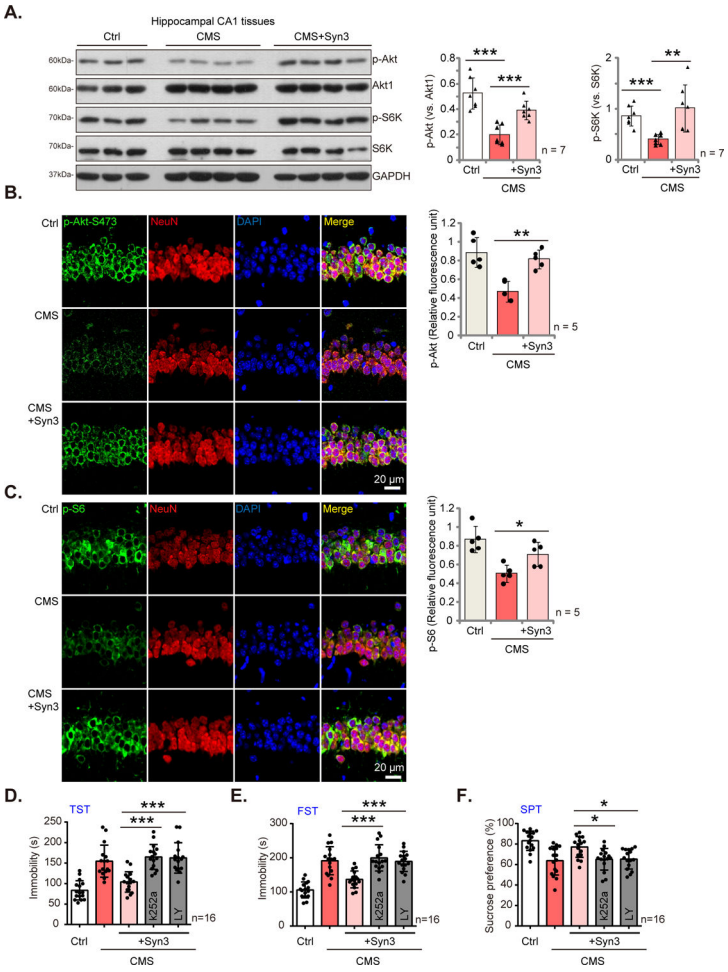

Figure 5. Syn3 restores Akt-mTOR activation in hippocampus of mice subjected to CMS.

(**A**) Effect of Syn3 on CMS-suppressed Akt and S6K phosphorylation. C57BL/6J mice with 5-week of CMS exposure were i.p. injected with Syn3 (1 mg/kg) for 12 hours, and the expression of Akt and S6K proteins in hippocampal CA1 region (stratum radiatum subregion) tissues examined by immunoblotting, and phosphorylation quantified (n = 7 stands for tissues of seven different mice in each group). (**B and C**) Effect of Syn3 on p-Akt and p-S6 immunofluorescence staining in CA1 neurons. Representative p-Akt (Ser^{473}) and p-S6 ($Ser^{235/236}$) fluorescence images in hippocampal CA1 brain sections were quantified from random views of sections from n = 5 mice in each group) were performed. (**D to F**) Effect of TrkB or PI3K-Akt-mTOR inhibition on Syn3's antidepressant-like activity. After 5 weeks of CMS exposure, C57BL/6J mice then underwent bilateral intrahippocampal infusion of K252a (1 ng in 0.5 μL per side) or LY294002 (5 ng/mL in 0.5 μL per side), followed by Syn3 administration (i.p., 1 mg/kg) for 12 hours, and performance in the TST (D), FST (E) and SPT (F) behavioral tests was assessed in n = 16 mice per group. Data are presented as mean ± SD. *$P < 0.05$, **$P < 0.01$, and ***$P < 0.001$ by one-way ANOVA plus Tukey's post hoc test.

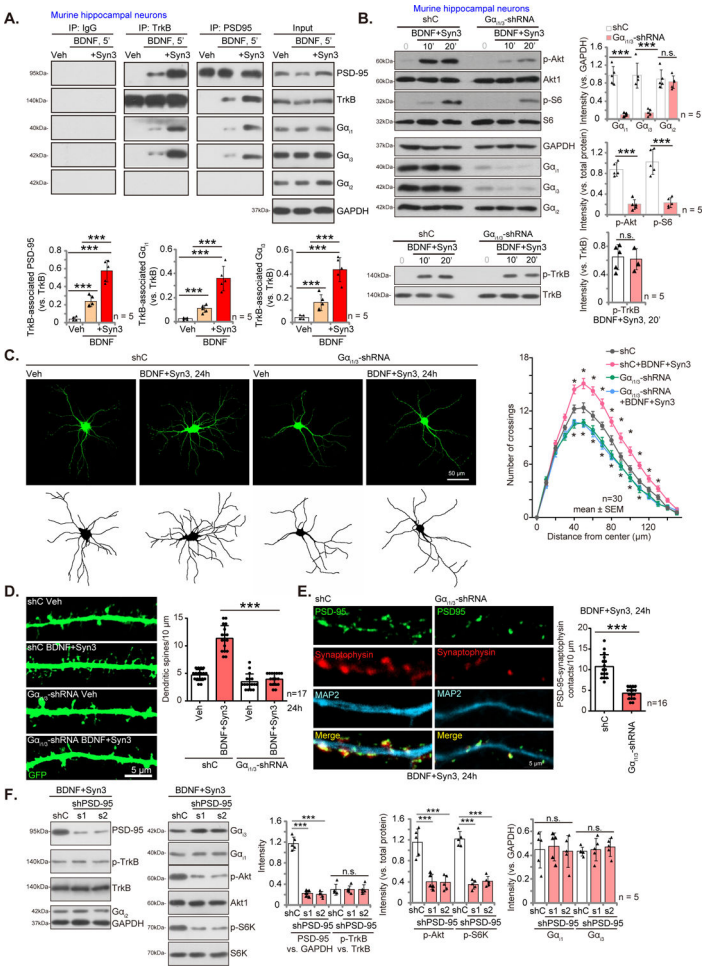

Figure 6. Syn3 facilitates BDNF-induced TrkB-PSD-95-G$\alpha_{i1/3}$ complex formation in hippocampal neurons.

(**A**) Co-immunoprecipitation (Co-IP) assays assessing the effect of Syn3 on TrkB-PSD-95-G$\alpha_{i1/3}$ association. Primary murine hippocampal neurons were treated with BDNF (25 ng/mL, 5 min) alone or after Syn3 (0.2 μM, 20 min pretreatment), followed by co-IP and immunoblotting. Expression of the indicated proteins was assessed in whole lysate “Input” and TrkB-associated PSD-95, Gα_{i1} and Gα_{i3} were quantified from n = 5 biological repeats. (**B**) Role of G$\alpha_{i1/3}$ in the effects of Syn3 on BDNF signaling. Primary hippocampal neurons transduced with the lentiviral Gα_{i1} shRNA plus lentiviral Gα_{i3} shRNA (G$\alpha_{i1/3}$-shRNA) or the lentiviral scramble control shRNA (shC) were treated with BDNF (25 ng/mL) after a pretreatment with Syn3 (0.2 μM, 20 min). The relative G$\alpha_{i1/2/3}$ protein expression and Akt/S6 phosphorylation was quantified in immunoblots from n = 5 biological repeats. (**C to E**) Role of G$\alpha_{i1/3}$ in the effects of Syn3 on dendritic branching (C, images of GFP-expression and Sholl analyses quantifying the number of crossings), spine formation (D, images and quantification of dendritic F-actin GFP-expression) and synaptic density (E, images and analysis of PSD-95–synaptophysin contacts). Primary hippocampal neurons were infected with lentiviral G$\alpha_{i1/3}$-shRNA or a lentiviral scramble control shRNA (shC), treated with BDNF (25 ng/mL) after Syn3 (0.2 μM, 20 min pretreatment) for 24 hours. Sholl analyses in (C) was performed on 30 neurons per group; the number of spines per 10-μm

dendrite in (D) was calculated from 17 neurons per group; and synaptic density in (E) was calculated from 16 neurons per group, each pooled from four independent experiments. (**F**) Effect of PSD-95 knockdown on the ability of Syn3 to enhance BDNF signaling. Primary hippocampal neurons transduced with the lentiviral PSD-95 shRNA (-s1/-s2) or the lentiviral scramble control shRNA (shC) were treated with BDNF (25 ng/mL) after Syn3 (0.2 μM, 20 min pretreatment), and total cell lysates were analyzed by immunoblotting for the indicated proteins, quantified from n = 5 biological repeats. Data are presented as mean ± SD. *$P <$ 0.05 vs. "shC" (C), ***$P < 0.001$, "n.s." not significant ($P > 0.05$) by one-way ANOVA plus Tukey's post hoc test (A, D and F), Student's *t* test (B and E), or two-way ANOVA with Sidak's post hoc test (C).

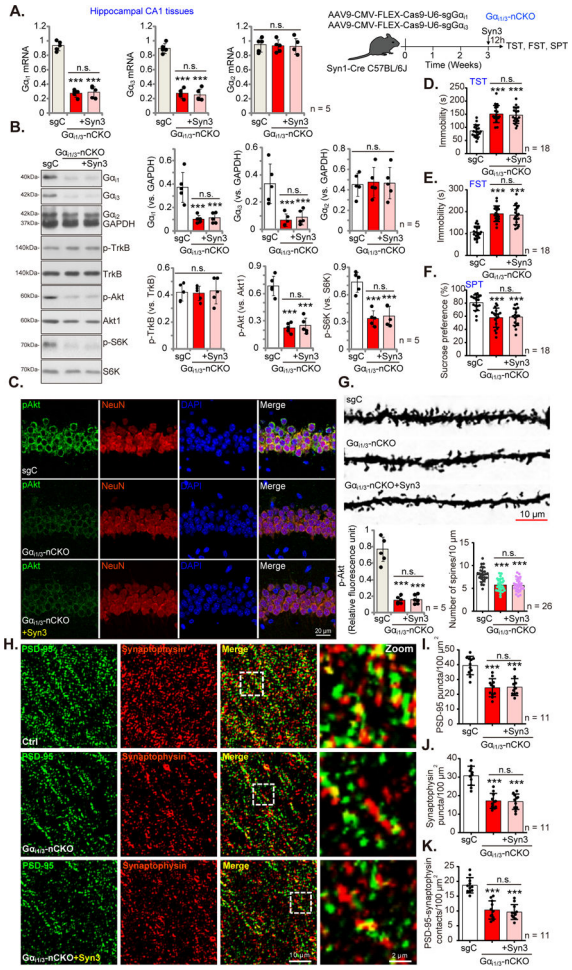

Figure 7. Syn3 fails to mitigate depression-like phenotypes in mice with neuronal conditional knockout of $G\alpha_{i1/3}$ in the hippocampus.

(**A to B**) Effect of $G\alpha_{i1/3}$ neuronal conditional knockout ($G\alpha_{i1/3}$-nCKO) on Syn3 signaling. Schematic, top right (A). AAV9-CMV-FLEX-Cas9-U6-sg$G\alpha_{i1}$ (0.25 μL/side) plus AAV9-CMV-FLEX-Cas9-U6-sg$G\alpha_{i3}$ (0.25 μL/side) were bilaterally injected into the CA1 region of the hippocampus of Syn1-Cre C57BL/6J mice, generating hippocampal $G\alpha_{i1/3}$-nCKO mice after three weeks. Control Syn1-Cre mice were injected with AAV9-CMV-FLEX-Cas9-U6-sgC (0.5 μL, "sgC"). $G\alpha_{i1/3}$-nCKO mice were injected with a single dose of Syn3 (1 mg/kg i.p.; pink bars) or not (red bars). mRNA expression (A) and protein abundance and phosphorylation by immunoblotting (B) 12 hours after Syn3 injection was quantified from n = 5 biological repeats. (**C**) Images and analysis of p-Akt (Ser^{473}) staining in hippocampal CA1 brain sections from mice described in (A-B), quantified in sections from n = 5 mice in each group. Scale bar, 20 μm. Analysis beside bottom-right merged image. (**D to F**). Performance of $G\alpha_{i1/3}$-nCKO mice described in (A) on the TST (D), FST (E) and SPT (F) behavioral tests. n = 18 mice per group. (**G**) Images of Golgi-stained dendritic spines in the hippocampal neurons from $G\alpha_{i1/3}$-nCKO mice (scale bar, 10 μm), with assessment of spine density (below images, right). Dendritic spines were counted from 30-μm-long dendritic segments located 50–80 μm from the soma of n = 26 randomly selected neurons from N = 6 to 7 mice per group. (**H to K**) Imaging analysis of synaptic density in the hippocampal

CA1 stratum radiatum subregion of $G\alpha_{i1/3}$-nCKO mice. The density of PSD-95 puncta (I), synaptophysin puncta (J) and PSD-95–synaptophysin contacts (K) were quantified in randomly-selected sections from n = 11 mice. Data are presented as mean ± SD. ***$P <$ 0.001 vs. “sgC” group, “n.s.” not signficant ($P > 0.05$) by one-way ANOVA plus Tukey’s post hoc test.

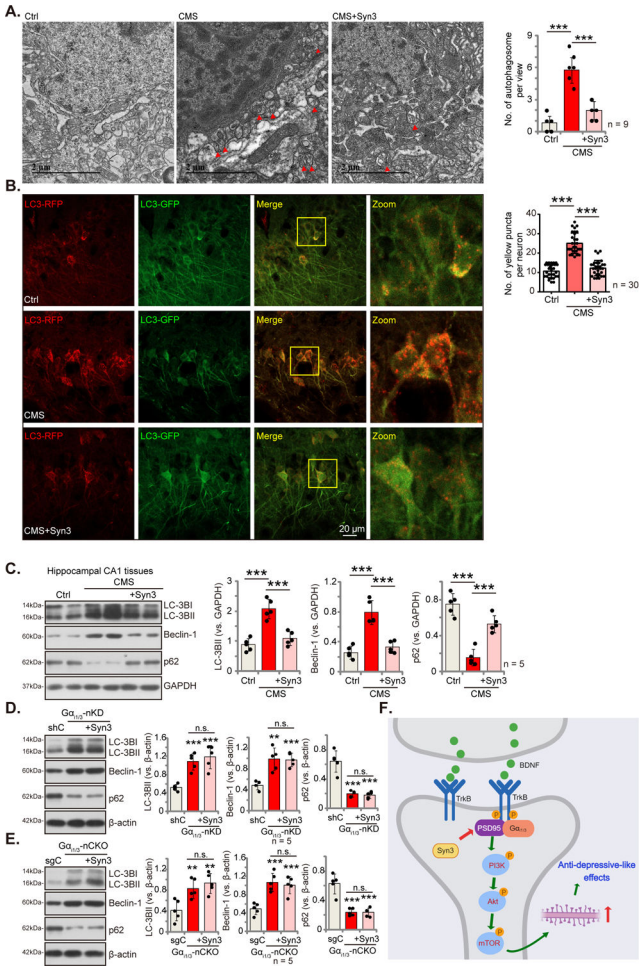

Figure 8. Syn3 ameliorates autophagy activation in hippocampal neurons following CMS.

(**A and B**) Autophagosome formation in the hippocampal CA1 region, assessed by electron microscopy (A) and immunofluorescence analysis of AAV-mRFP-GFP-LC3 reporter (B), in mice exposed to 5 weeks of CMS assessed 12 hours after i.p. injection with a single injection of Syn3 (1 mg/kg). Autophagosome quantification in (A) was performed in randomly selected hippocampal neurons from n = 9 mice per group, and from n = 30 randomly selected neurons from six mice each group in (B). (**C to E**) Western blotting of hippocampal tissues for markers of autophagic flux in mice after CMS exposure (C) and in $G\alpha_{i1/3}$ nKD mice (D) and $G\alpha_{i1/3}$ nCKO mice (E), after treatment with Syn3 (i.p. 1 mg/kg, 12 hours), from n = 5 mice per group. ***$P < 0.001$ (A to C); ***$P < 0.01$, **$P < 0.01$ vs. “shC”/“sgC” tissues (D and E); “n.s.” not significant ($P > 0.05$; D and E), by one-way ANOVA plus Tukey’s post hoc test. (**F**) The proposed signaling mechanism derived from this study. PSD-95, a master synaptic scaffold protein, complexes with TrkB to amplify BDNF signaling. In response to BDNF, PSD-95 associates with TrkB to recruit $G\alpha_{i1/3}$ resulting in amplification of PI3K-Akt-mTOR signaling. Syn3 facilitates BDNF-induced TrkB-PSD-95-$G\alpha_{i1/3}$ complex formation to restore Akt-mTOR activation in mice subjected to CMS to increase neurite outgrowth and dendritic spine formation in murine hippocampal neurons.